INL/RPT-22-66788-Revision-0

Thermal Ratcheting Analysis of TEDS Packed-bed Thermocline Energy Storage Tank - Modeling Methodology and Data Validation

May 2022

Sunming Qin, Jun Soo Yoo, Terry James Morton

Changing the World's Energy Future

Idaho National Laboratory

INL is a U.S. Department of Energy National Laboratory operated by Battelle Energy Alliance, LLC

INL/RPT-22-66788-Revision-0

Thermal Ratcheting Analysis of TEDS Packed-bed Thermocline Energy Storage Tank - Modeling Methodology and Data Validation

Sunming Qin, Jun Soo Yoo, Terry James Morton

May 2022

Idaho National Laboratory
Idaho Falls, Idaho 83415

http://www.inl.gov

Prepared for the
U.S. Department of Energy
Under DOE Idaho Operations Office
Contract DE-AC07-05ID14517

INL xxx-xx-xxxxx
Revision 0

Thermal Ratcheting Analysis of TEDS Packed-bed Thermocline Energy Storage Tank

Modeling Methodology and Data Validation

April | 2022

Sunming Qin
Idaho National Laboratory
JunSoo Yoo
Idaho National Laboratory
Terry J. Morton
Idaho National Laboratory

IES
Integrated Energy Systems

INL is a U.S. Department of Energy National Laboratory operated by Battelle Energy Alliance, LLC

INL xxx-xx-xxxxx
Revision 0

Thermal Ratcheting Analysis of TEDS Packed-bed Thermocline Energy Storage Tank

Modeling Methodology and Data Validation

Sunming Qin
Idaho National Laboratory
JunSoo Yoo
Idaho National Laboratory
Terry J. Morton
Idaho National Laboratory

April* | *2022

Idaho National Laboratory
Integrated Energy Systems
Idaho Falls, Idaho 83415

http://www.ies.inl.gov

Prepared for the
U.S. Department of Energy
Office of Nuclear Energy
Under DOE Idaho Operations Office
Contract DE-AC07-05ID14517

Page intentionally left blank

SUMMARY

This report investigates numerical modeling methods for thermal ratcheting analysis of packed-bed thermal energy storage (TES) tank and discusses the validation results via comparison with experimental data. The experimental data obtained from various design characteristics of packed-bed thermocline tanks, including the Thermal Energy Distribution System (TEDS) TES tank at Idaho National Laboratory (INL), were used to validate thermal and mechanical models developed in this study to evaluate the thermal ratcheting potential. The thermal model was shown to predict the transient thermal propagation through the packed-bed thermocline tanks generally well. However, a larger discrepancy was observed during the comparison with the data from TEDS, presumably due to the uncertainty of boundary conditions given from the experiment. Based on the comparative study between the thermal model predictions and experimental data of various packed-bed thermocline tanks, potential improvements were suggested for the future TEDS experiments for more precise validation study.

For mechanical (thermally induced stress) analysis, two different modeling approaches were tested to evaluate hoop stress applied to the packed-bed TES tank wall, which is a major cause of thermal ratcheting process: (i) infinite rigidity model and (ii) Drucker-Prager (DP) model. The ‘model (i)’ is a conservative method with infinite rigidity assumption of granular filler inside a TES tank, whereas the ‘model (ii)’ is a method that takes into account more realistic processes such as thermal expansion of filler and tank wall as well as inter-particle interactions during the cyclic operation of a packed-bed TES tank. The validity of each modeling method was examined by comparing the numerical simulation with the experimental data obtained from the packed-bed TES tank for Solar One pilot plant. Then, the effects of various model parameters were discussed to evaluate the thermal ratcheting potential of the TEDS TES tank. The preliminary thermal ratcheting analysis implies that the TEDS TES tank will hold its structural integrity during the normal operation cycles.

Page intentionally left blank

CONTENTS

FIGURES

TABLES

Page intentionally left blank

ACRONYMS

Bi	Biot Number
C_p	Specific heat [J/kg-K]
CFD	Computational Fluid Dynamics
D	Diameter [m]
D_{in}	Inner Diameter of Tank [m]
D_e	Equivalent (or Effective) Diameter [m]
EOS	Equation of State
h_b	Height of porous bed [m]
INL	Idaho National Laboratory
k	Thermal Conductivity [W/m-K]
$m_{f,in}$	Inlet Mass Flow Rate [kg/s]
Pe	Peclet Number
T	Temperature [°C]
T_f	Fluid Temperature [°C]
TEDS	Thermal Energy Distribution System
TES	Thermal Energy Storage
U_f	Fluid Velocity [m/s]
$U_{f,avg}$	Average Fluid Velocity [m/s]

Greeks

ρ	Density [kg/m^3]
v	Kinematic Viscosity [m^2/s]
	Time Scaling Factor

Page intentionally left blank

Thermal Ratcheting Analysis of TEDS Packed-bed Thermocline Energy Storage Tank

Modeling Methodology and Data Validation

1. Introduction

Dynamic Energy Transport and Integration Lab (DETAIL) has been built at Idaho National Laboratory for experimental demonstration and validation research on Nuclear-Renewable Hybrid Energy System [1]. The thermal energy distribution system (TEDS) is a thermal-hydraulic flow loop with its own dedicated control system to support the integration of co-located multiple experimental systems in DETAIL, where a packed-bed thermal energy storage is installed. The packed-bed thermal energy storage is adopted in TEDS because it offers a low-cost single-tank thermal storage option compared to the traditional two-tank thermal storage. However, the thermo-mechanical issue like thermal ratcheting of the tank wall may pose a significant design concern unless it is carefully addressed. Thermal ratcheting is caused by the rearrangement of granular filler inside a packed-bed tank during continuous thermal cycling operation of the packed-bed thermocline tank. If the thermally induced stress exceeds yield strength of the tank wall, it may cause catastrophic consequences like rupture of the thermal storage tank. Thus, it is crucial to understand the phenomenon to ensure robust operation of packed-bed energy storage system.

This report investigates numerical modeling methods for thermal ratcheting analysis of packed-bed thermocline TES tank. A one-way coupled method is employed for the thermo-mechanical analysis of packed-bed thermocline tank to evaluate the thermal ratcheting potential. For the validation of thermal model, experimental data from various design characteristics of packed-bed thermocline tanks, obtained during charge and discharge operation cycles, are used. For mechanical (or stress) analysis, two different modeling approaches are tested to evaluate hoop stress applied to the packed-bed tank wall, which is a major cause of thermal ratcheting: (i) infinite rigidity model and (ii) Drucker-Prager (DP) model. The ‘model (i)’ is a conservative method with infinite rigidity approximation of granular filler inside a TES tank, whereas the ‘model (ii)’ is a method that considers more realistic physical processes such as thermal expansion of solid filler and tank wall as well as inter-particle interactions during thermal cycling operation of a packed-bed TES tank. The validity of each modeling method is examined by comparing the simulation results with experimental data. Specifically, strain gage data obtained from the operation of the packed-bed thermocline tank for Solar One pilot plant [2] are used for the validation. Then, model parametric study is performed to discuss the thermal ratcheting potential of the packed-bed thermocline tank for Idaho National Laboratory’s (INL) thermal energy distribution system (TEDS) [3].

The details of target problems of present study, thermal and structural modeling methods for thermal ratcheting analysis, and numerical analysis and validation results are described in the following sections.

2. Experimental Database

The present modeling and validation study is performed by comparing the numerical simulations of packed-bed thermocline energy storage device with experimental data. For the thermal model validation, the thermal measurement data obtained by Esence et al. [4], Pacheco et al. [5], and INL (TEDS experiment) [6], from the various design characteristics of packed-bed thermocline tanks, were employed. It is noted that the thermal model developed and validated in this study is used to provide adequate thermal boundary conditions for the stress analysis along the packed-bed thermocline tank during the thermal cyclic operation of the packed-bed TES tank. Table 1 compares the design characteristics of the packed-bed thermocline tanks used for the validation of the present thermal modeling approach for the thermal ratcheting study. Regarding the TEDS experiment, the packed-bed thermocline tank has been instrumented with multiple thermocouples as well as strain gages to detect axial and radial temperature distribution, tank wall temperature, and thermal strain as shown in Figure 1, and some experimental data were recently acquired during the startup and commissioning testing [6]. In this study, the thermal data acquired using TEDS were compared with the computational model predictions not only for validating both the thermal model, but also for suggesting the potential improvement from the experimental point of view for more precise validation studies in the future. Details of the TEDS experimental data used for the present work is described in Ref. [6].

For the stress analysis and model validation study, two packed-bed thermocline TES tanks of different scales, used in conjunction with (i) Solar One pilot plant [2, 7] and (ii) INL Thermal Energy Distribution System (TEDS) [3], were adopted. The two packed-bed thermocline tanks for Solar One and TEDS, respectively, have different design characteristics in terms of scale (i.e., tank size and energy storage capacity), tank shape (i.e., height-to-diameter ratio), filler material and size, heat transfer fluid, and operation temperature during cyclic charge and discharge processes. In Table 2, the basic design characteristics of the two TES tanks are briefly compared, which are used in the numerical models of the two packed-bed TES tanks for the thermal ratcheting analysis. The thermal and stress measurement data obtained from Solar One thermocline tank are available in Refs. [8, 9].

3. Problem Description

The physical problem of primary interest is the thermally induced stress behavior during the cyclic charge and discharge processes of the packed-bed thermocline tank, which may cause thermal ratcheting. The stress behavior is closely related to the transient thermal behavior, thus it is important to accurately understand and evaluate the thermal response of the packed-bed thermocline tank in order to achieve correct insight into the thermal ratcheting potential. As such, the validations of both thermal and stress models have been conducted in this study by comparing the model predictions with the experimental data acquired from the thermal cycling operation of packed-bed thermocline tanks.

In a charge (or heat storage) period of packed-bed thermocline tank, hot fluid from a heat source is charged into the tank from the top while cold fluid exits from the bottom. In a discharge period, hot fluid is discharged from the top of the tank to heat customers while cold fluid, which is cooled through the energy extraction cycle, comes into the bottom of the tank. Thus, hot fluid is always present over cold fluid during the operation of packed-bed thermocline tank due to the density difference, which prevents convective mixing of the fluids. The thermal and stress behaviors under this typical operation cycle of a packed-bed thermocline tank, and how to analyze them, are the problem of current interest, for which thermal and stress models were developed and the model predictions were compared with the experimental data from various design characteristics of packed-bed thermocline tanks including TEDS.

Table 1. Design characteristics of packed-bed thermocline systems used for thermal model validation

	Esence et al.	**Pacheco et al.**	**INL TEDS**
Storage Capacity	-	2.3 MWh_{th}	200 kWh_{th}
Tank shape (D_{in} / h_b)	Cylindrical (1.0 m / 3.0 m)	Cylindrical (3.0 m / 5.2 m)	Cylindrical (0.88 m / 3.55 m)
Tank wall material	Stainless steel	Carbon steel	Carbon steel
Filler material	Silica gravel and silica sand	Quartzite rock and silica filter sand	Alumina bead
Bed porosity	0.27	0.22	0.4
Heat transfer fluid	Therminol® 66	Nitrate Salt (50%wt $NaNO_3$+50%wt KNO_3)	Therminol® 66
Operation temperature	85 - 150 °C	290 - 396 °C	225 - 325 °C

Table *2*. Packed-bed thermal energy storage tanks for Solar One and INL TEDS

	Solar One	**INL TEDS**
Storage Capacity	170 MWh_{th}	200 kWh_{th}
Tank shape (D_{in} / h_b*)	Cylindrical (18.2 m / 12.4 m)	Cylindrical (0.88 m / 3.55 m)
Tank wall material	Carbon steel	Carbon steel
Filler material	Sand and rock mixture ($D_{e,sand}$=0.2 cm, $D_{e,rock}$=5 cm)	Alumina bead (D=0.32 cm)
Bed porosity	0.4 (monodisperse layer) 0.22 (mixture layer)	0.4
Heat transfer fluid	Caloria oil	Therminol® 66
Operation temperature	204 - 304 °C	225 - 325 °C

* Here, the tank height only considers the length filled with granular filler (i.e., sand/rock mixture for Solar one, and spherical particles made of alumina for TEDS). Inside the thermocline tank for Solar One, the two distinct types of granular fillers (i.e., sand and rock) are stacked from the tank floor in the following order: a 0.3 m layer of sand, a 1.1 m layer of rock, a 10.5 m layer of rock/sand mixture, and a 0.5 m layer of rock [8].

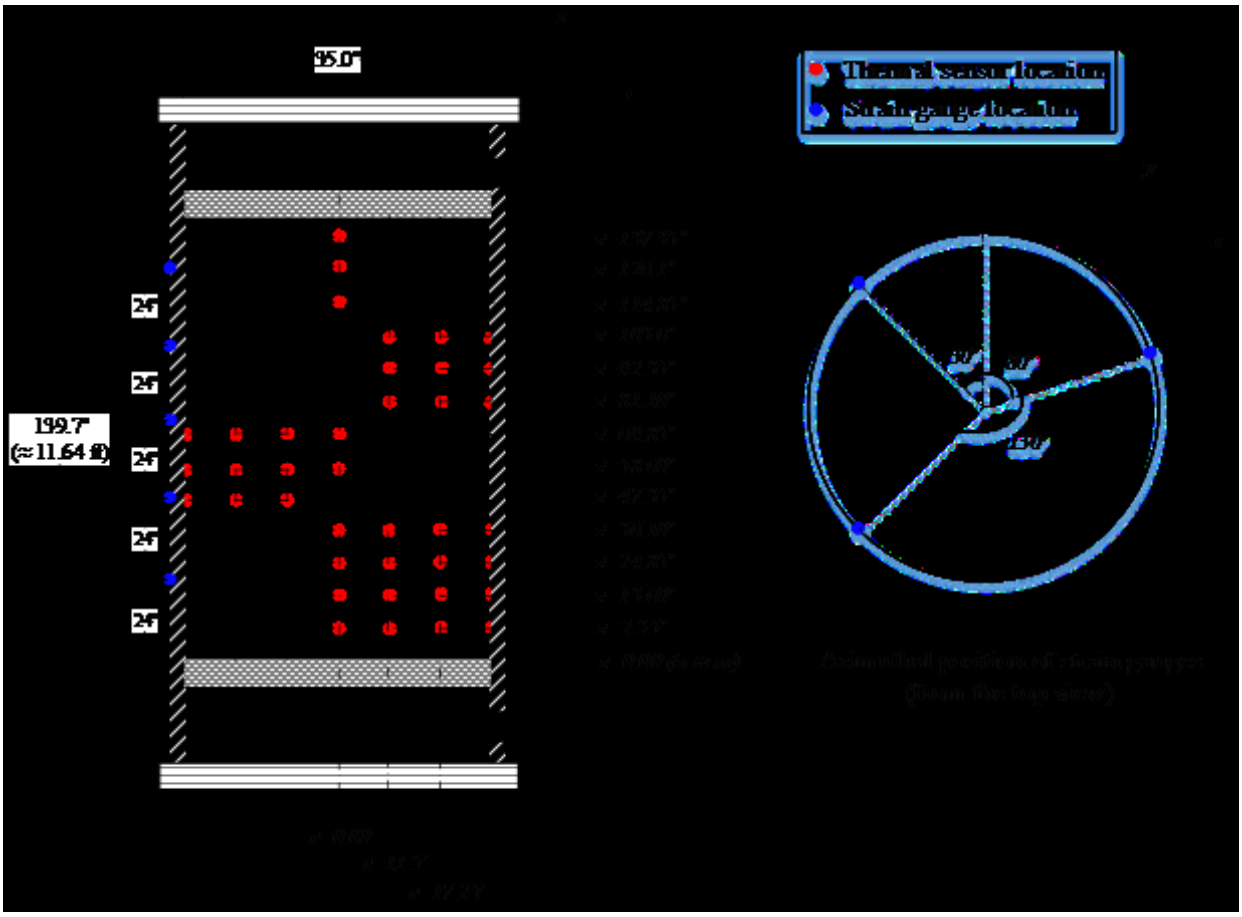

Figure 1. Location of thermal and stress sensors installed in INL TEDS packed-bed thermocline tank

Packed-bed Thermocline Tank for Solar One Plant

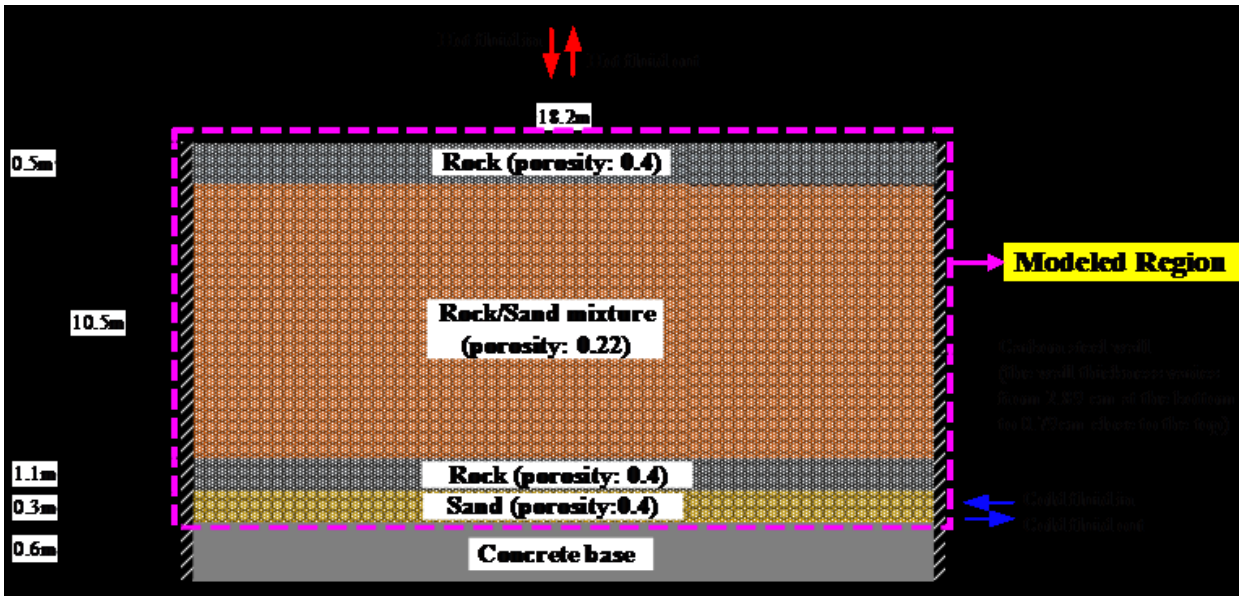

Packed-bed Thermocline Tank for INL TEDS

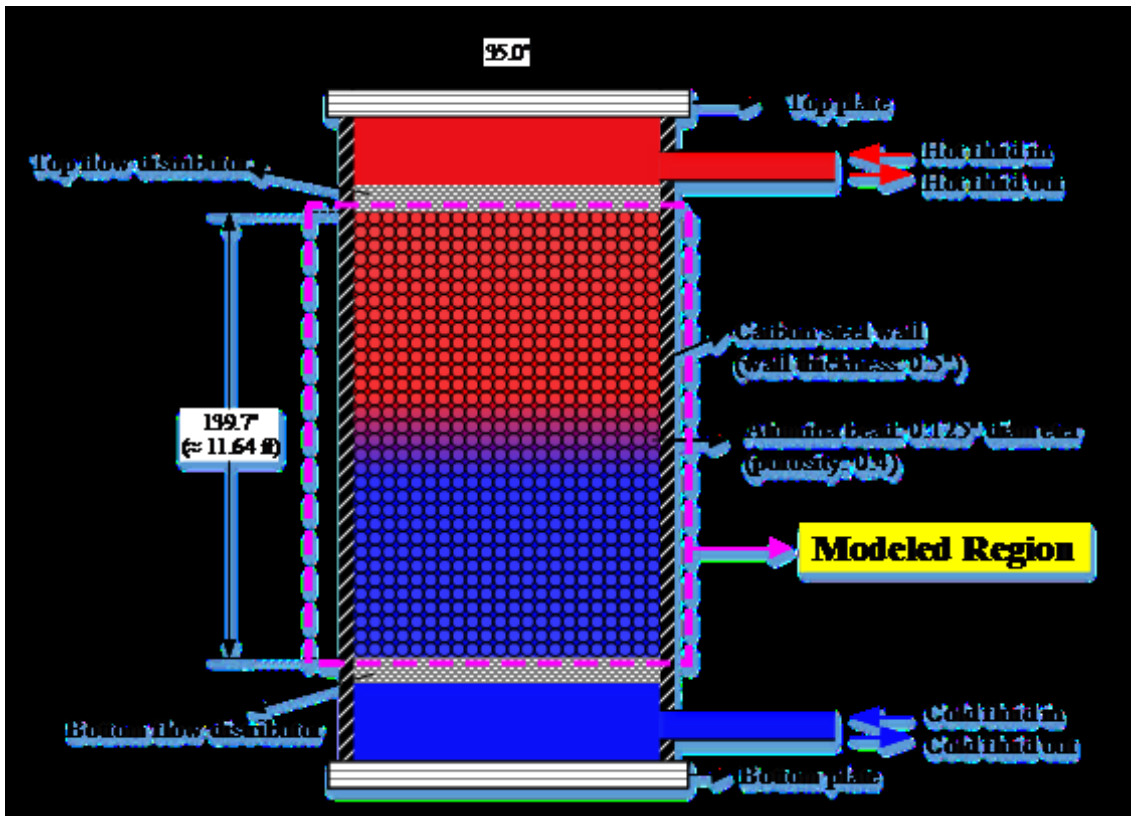

Figure 2. Design characteristics and associated modeling geometries of packed-bed thermocline tanks for Solar One pilot plant (top) and INL TEDS (bottom)

4. Numerical Modeling Method

The thermal ratcheting is caused by complex interaction of thermal transport in the porous bed and solid mechanics during the cyclic operation of packed-bed thermocline tank, thus it requires a coupled thermal and stress analysis. The present study employs a one-way coupled method for the thermo-mechanical analysis of the packed-bed thermocline tank to evaluate thermal ratcheting potential. In this modeling approach, the thermal and mechanical models are solved independently, and the transient thermal solutions are used as boundary conditions at each time step of the transient mechanical analysis. This assumes that the transient thermal solution causes thermal-induced strains, but the effect of mechanical deformation or displacement on the thermal response is neglected. This is an efficient and widely-used approach when the purpose of analysis is to determine thermo-mechanical stresses and associated structural deformation in the absence of evolving contact between components [10].

This section describes thermal and mechanical analysis models and methods applied to the present thermal ratcheting study for the packed-bed thermocline tank. To validate the thermal and mechanical modeling approaches employed in this study, comparisons were performed between simulations and experimental data available in the literature. Then, the thermal and stress analysis models for the TEDS thermocline tank were developed.

4.1 Thermal model

A two-dimensional (2-D) porous media modeling approach was employed to simulate the transient thermal behavior of packed-bed thermocline tank. The commercial CFD software, STARCCM+ version 15.06, was used to develop the thermal models. A transient laminar flow solver was adopted in consideration of the Reynolds number determined by the fluid velocity, characteristic length scale of the porous bed, and fluid's thermal properties for the test problems used in this study.

Figure 3 shows meshing strategy commonly applied to the multiple CFD simulations of the packed-bed thermocline tanks during this study. The domain was discretized with quadrilateral type mesh and included outer tank wall to account for the wall influence on the thermal response of the porous bed during the charging and discharging processes. Also, the prism layer type finer mesh was applied at the near-wall region to better capture the velocity profile close to the wall.

To address the thermal transfer within a porous bed, the porous media thermal non-equilibrium model was employed, where the fluid and porous phase each have their own temperature, rather than being treated as a homogeneous mixture, and the heat transfer occurs based on the temperature difference between the fluid and the porous phase. The heat transfer coefficient and interaction surface area to determine the heat transfer between the fluid and the porous phase were obtained using the correlation employed by Lew et al [11] and originally provided by Nelis and Klein [12]. The heat transfer coefficient for the wall thermal loss was determined as suggested by Esence et al (2019) [4].

The transient simulation was performed with a time step size of 1.0 sec. The numerical solution at each time step was considered converged when the scaled residuals of the mass, momentum, and energy equation were reduced to 10^{-4}, 10^{-4}, and 10^{-6}, respectively.

The initial and boundary conditions of all the CFD simulation cases, such as initial temperature distribution along the packed-bed TES tank and transient inlet mass flow rate (or fluid velocity), were applied based on the experimental measurements. Also, to correctly model the transient thermal response of the porous medium during the charging and discharging processes, temperature-dependent material properties were implemented as user defined functions.

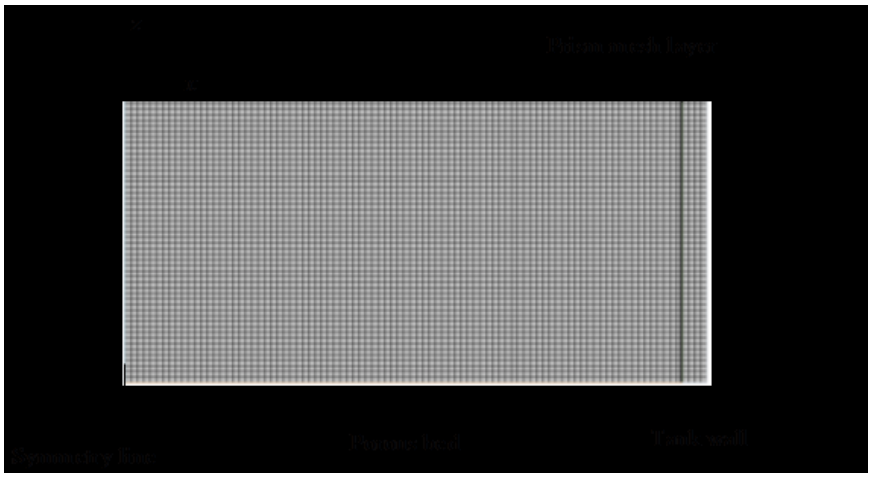

Figure 3. 2-D mesh strategy for the present CFD simulation of packed-bed thermocline tank

The relevant modeling assumptions applied to the present CFD models, i.e., thermal models, for the transient thermal analysis of the packed-bed TES thermocline tank are summarized as follows:

(i) The fluid flow through the porous bed is incompressible.

(ii) Temperature-dependent properties of the fluid, filler particles, and tank wall are considered.

(iii) Porosity is constant across the porous bed.

(iv) The heat conduction inside the filler particles is neglected (Bi <0.1). Note, however, that the thermal diffusion across the porous bed and the heat transfer between the fluid and filler particles are addressed using the effective thermal conductivity and heat transfer coefficient, respectively.

(v) The effect of radiation heat transfer is neglected due to the relatively low operating temperature of the packed-bed thermocline tanks subjected to the current study.

With the transient thermal modeling approach for the packed-bed thermocline tank described above, the CFD model predictions were compared with the experimental data obtained by Esence et al. [4] and Pacheco et al. [5] to validate the current thermal modeling approach. It is noted that the experiment performed by Esence et al. [4] used the same working fluid as TEDS (Therminol® 66) with a packed-bed thermocline tank of similar dimensions (operating temperature range: 90 - 150 °C), while the experiment by Pacheco et al. [5] was performed with much larger scale of thermocline tank using molten salt as the working fluid (operating temperature range: 290 - 400 °C). For more detailed information of these experiments, readers are advised to refer to the Refs. [4, 5].

The comparison between the present CFD model predictions and the experimental data acquired from the two different characteristics of packed-bed TES experiments is shown in Figure 4 and Figure 5. Figure 4 and Figure *5* presents that the thermal front evolution during the charging and discharging processes of the packed-bed thermocline tanks is predicted quite well by the current modeling approach, regardless of the inlet boundary conditions (e.g., inlet fluid velocity) and tank scales tested during this study.

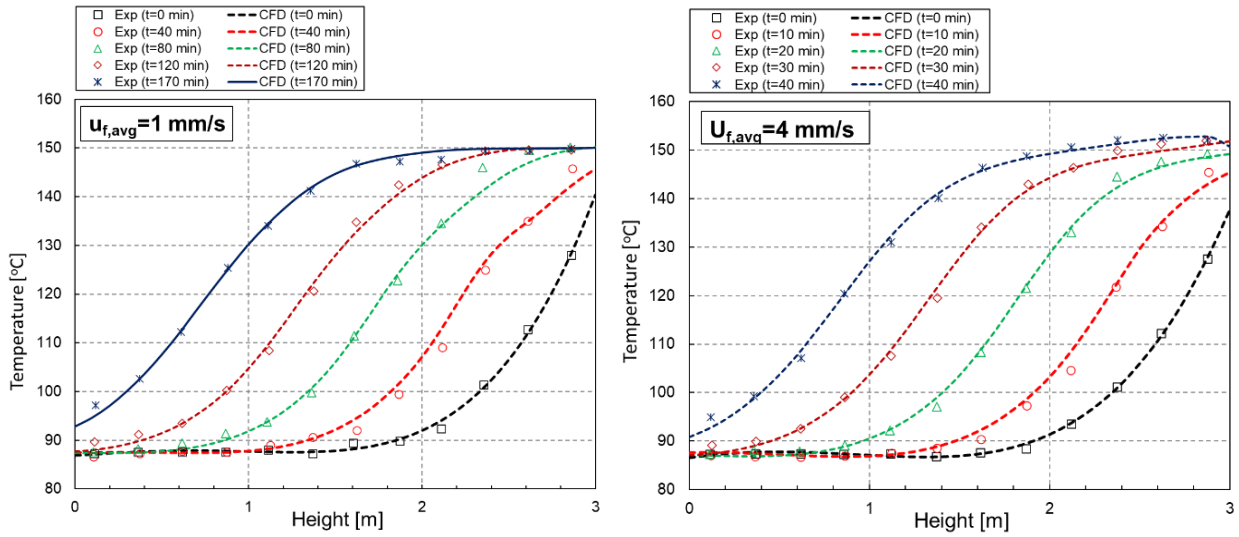

Figure 4. Comparison of fluid temperature evolution during a charging mode between CFD simulation and experimental measurement by Esence et al. (2019) [4]

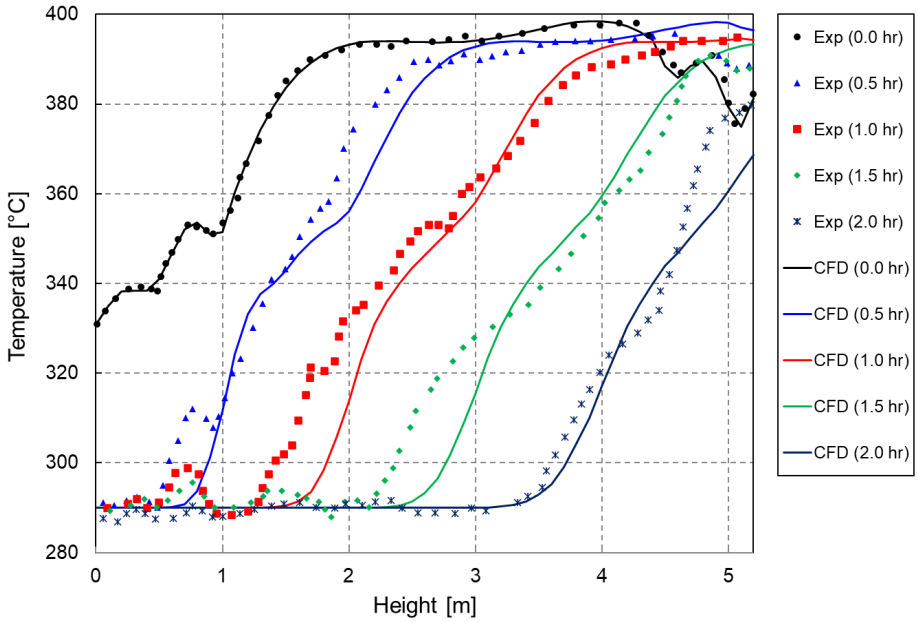

Figure 5. Comparison of fluid temperature evolution during a discharge mode between CFD simulation and experimental measurement by Pacheco et al. (2002) [5]

Using the modeling strategy that yielded the validation results presented in Figure 4 and Figure 5, a CFD model (i.e., thermal model) was developed for the TEDS thermocline tank. Although the current data obtained from TEDS are somewhat preliminary in terms of limited TES operation scenario and data sampling procedure, the comparative study between CFD simulation and TEDS data was performed in an effort to identify the potential improvements in the future experiment for more precise validation research as well as to verify the performance of the computational models developed in this study. In Figure 6, the CFD predictions for the transient evolution of the temperature profile along the TES tank is compared with the experimental data during the charge (top) and discharge (bottom) operation modes of the TEDS

TES tank. It is noted that due to the highly fluctuating characteristics of the raw data, the exact inlet boundary conditions of the experiment, such as transient inlet mass flow rate, could not be applied to the CFD model. This results in the greater discrepancy between the CFD predictions and the experimental data as shown in Figure 6, relative to the comparison shown in Figure 4 and Figure 5. In other words, the discrepancy between the CFD prediction and the TEDS experimental data shown in Figure 6 is mainly attributable to the substantial uncertainty of the boundary conditions applied to the simulation, including the inlet mass flow rate, inlet fluid temperature, and wall thermal loss rate.

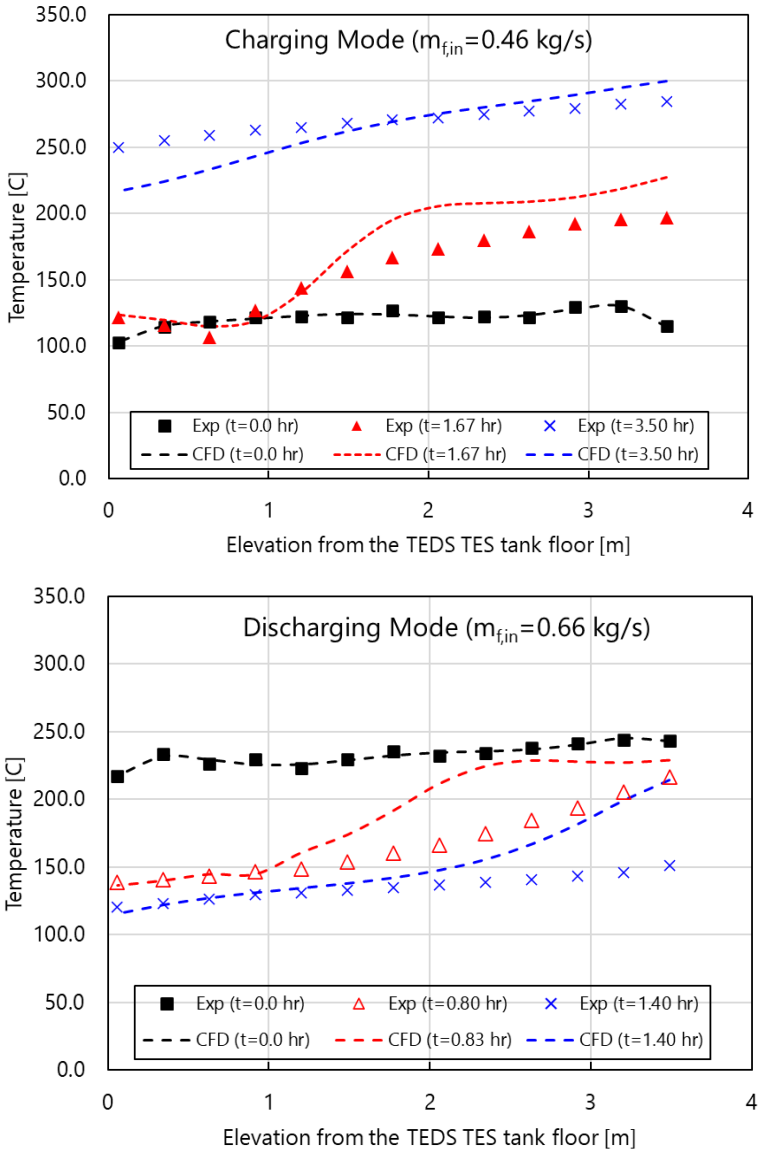

Figure 6. Comparison of fluid temperature evolution between CFD simulation and experimental measurement during charge and discharge modes of TEDS TES tank

During the validation studies shown in Figure 4 and Figure 5, it was learned that the current model prediction results were substantially sensitive to the boundary conditions such as transient inlet flow rate and transient inlet fluid temperature. Thus, it is very important to apply the well-defined (transient)

boundary conditions measured from experiments in order to precisely predict the thermal field propagation across the porous bed and tank wall from the present modeling approach.

During the data analysis for the comparative study between CFD (thermal model) predictions and TEDS data, several items to be addressed for the future TEDS experiment were observed:

(i) An optimal data sampling strategy seems to be needed to better capture the physical processes occurring in TEDS. Currently, data is collected at a rate of once per second, which can lead to substantial fluctuations with noise signal (e.g., inlet mass flow rate), making it difficult to define representative boundary conditions for precise validation study.

(ii) An inconsistency was noticed for some thermal measurements. For example, the thermal sensors installed at the centerline of the TES tank tend to detect lower temperature compared to those close to the tank wall. This may be due to the channeling that leads the hot fluid from the top of the thermocline tank to flow towards the walls of a porous bed. However, the temperature difference existed even before the fluid started flowing through the tank, indicating that there might be an issue, such as calibration, with the thermal sensors installed at the centerline. During the next service outage for TEDS, all thermocouples should be calibrated.

(iii) The measurement uncertainties for the relevant physical parameters, such as transient inlet mass flow rate and inlet temperature into the TES tank, need to be better defined (quantitatively), which may require additional repeatability tests.

These improvements for future TEDS experiments will allow more precise validation of the computational models when data become available from the various operating modes of TEDS.

Table 3. Thermophysical properties for thermal analysis of Solar One TES tank

Material	**ρ [kg/m^3]**	**k [W/m-K]**	**C_p [J/kg-K]**	**ν [m^2/s]**
Carbon steel wall [9]	7850.0	47.0	475.0	-
Caloria HT-43 mineral oil	Temperature-dependent [9, 13]	Temperature-dependent [9, 13]	Temperature-dependent [9, 13]	Temperature-dependent [9, 13]
Rock/sand mixture [14]	2643	2.2	1000.5	-

Table 4. Thermophysical properties for thermal analysis of INL TEDS TES tank

Material	**ρ [kg/m^3]**	**k [W/m-K]**	**C_p [J/kg-K]**	**ν [m^2/s]**
Carbon steel wall	7850.0	47.0	475.0	-
Therminol® 66	Temperature-dependent [15]	Temperature-dependent [15]	Temperature-dependent [15]	Temperature-dependent [15]
Alumina (filler) [16]	3950	Temperature-dependent [16]	Temperature-dependent [16]	-

4.2 Mechanical model for thermal stress analysis

With the thermal data acquired from the thermal analysis and experiment, described in Section 3 and 4.1, the stress analysis was performed to investigate the thermal ratcheting potential of the packed-bed thermocline tank using the commercial software Abaqus 2018.HF3 [17]. This section describes two different modeling approaches, (i) infinite rigidity model and (ii) Drucker-Prager model, employed in this study for the thermal stress analysis during the cyclic operation of the packed-bed thermocline tank.

4.2.1 Infinite rigidity model

This is a simplified modeling approach that assumes the filler material inside a TES tank is infinitely rigid. This approach is implemented by fixing the inner tank wall in the radial direction to prevent the tank from contracting during the simulation of discharge cycle while allowing the tank to expand freely with the temperature increase during the charge cycle. Given the fact that the infinite rigid model only requires the tank geometry without filler material inside, the material properties and stress-strain data for the TES tank wall (made of carbon steel) are needed as shown in Table 5 and Table 6. Abaqus/Standard module, which is a general-purpose Finite-Element analyzer that employs implicit integration scheme, is used with the infinite rigidity model setup.

Table 5. Material properties of carbon steel [9] used for the TES tank models

Conductivity (W/m-K)	47
Density (kg/m^3)	7850
Young's modulus (GPa)	140
Poisson's ratio	0.3
Thermal expansion coefficient (μm/m-K)	13
Specific heat (J/kg-K)	475

Table 6. Stress-strain data for carbon steel [9] used for the TES tank models

True strain	True stress (MPa)
0	400
0.02	458
0.04	492
0.06	514

4.2.2 Drucker-Prager (DP) model

Drucker-Prager (DP) model was proposed by Drucker and Prager [18] in 1952. This model can be used to represent frictional interactions between granular solid particles in a continuum through shear-normal stress relation. This is an efficient way to mimic interaction among granular fillers in packed-bed TES tank more realistically under thermal cycling conditions while avoiding full simulation of inter-granular process. Abaqus/Explicit module, which employs explicit integration scheme to solve highly nonlinear systems with many complex contacts under transient loads, is utilized together with the DP modeling approach to take into account the interactions between the filler and tank during the thermal ratcheting process.

Due to the lack of filler beds' property data for the Solar One Plant (gravel/sand mixture) and TEDS (alumina beads), most parameters will need to be estimated from literature that deals with similar filler mixtures. Inspired by the work performed in González et al. [19], we implemented the stress-strain data measured using triaxial tests on the mixture of quartzite/silica in water. For the TEDS simulation, the same DP parameters as the Solar One Plant simulation were implemented in the filler modeling. TEDS-specific parameters need to be explored and investigated as the future model development work.

Table 7. Bed (filler materials) properties for the Solar One Plant and TEDS

Filler Material Properties	Solar One Plant	TEDS
Conductivity (W/m-K)	2.2 [19]	5.85
Density (kg/m^3)	2643 [19]	3950
Shear modulus (MPa)	75	
Specific heat (J/kg-K)	1000 [19]	1117
Internal angle of friction (deg)	34 [20]	
Dilatancy angle (deg)	28 [20]	
Flow stress ratio	0.778	

Table 8. Input parameters for equation of state (EOS) used for bed properties [21]

Filler EOS Parameters	Solar One Plant	TEDS
Bulk speed of sound: c_0 (m/s)	1450	
Linear coefficient: s	1.62	
Grüneisen's gamma: Γ_0	2	

Table 9. Strain-stress database for DP hardening of bed properties [20]

Strain	Stress (MPa)
0	1.034
0.01	0.35

0.02	0.49
0.04	0.52

Since Abaqus/Explicit [22] is known as a special-purpose Finite-Element analyzer that employs explicit integration scheme to solve highly nonlinear systems with many complex contacts under transient loads, the coupled temperature-structure simulation with the charge and discharge cycle can easily take several days to finish. In order to speed up the thermal-stress simulation and save the computational cost, investigations need to be conducted for scaling method to reduce the computational time while maintaining the simulation accuracy. Therefore, adopting time scaling method in the coupled temperature-structure analysis is proposed in this study to minimize the computation time.

Specifically, in order to apply the time scaling method, the thermal loads will be scaled by adjusting the related thermal coefficients to maintain the consistency of heat transfer behavior in the scaled simulation. Hammelmüller and Zehetner [23] modified the thermo-elastic equations by introducing the fictitious time and the fictitious specific heat , the modified equations can be presented as Equation (1) and (2):

(1)

(2)

where $\boldsymbol{E}$ is the linear strain tensor, $\boldsymbol{u}$ is the displacement vector, is the time scaling factor, k is the conductivity, the density, α the thermal expansion coefficient, λ and μ are Lamé coefficients, T is the actual temperature, T_0 the reference temperature, and the operator tr($\boldsymbol{A}$) denotes the trace of the given matrix $\boldsymbol{A}$. To investigate different settings of the time scaling factor for the metal forming process, Hammelmüller and Zehetner found that the Abaqus analysis can be run much faster without loss of accuracy as shown in Figure 7. However, they also noticed that the results with a relatively large scaling factor damped initially and take longer to converge.

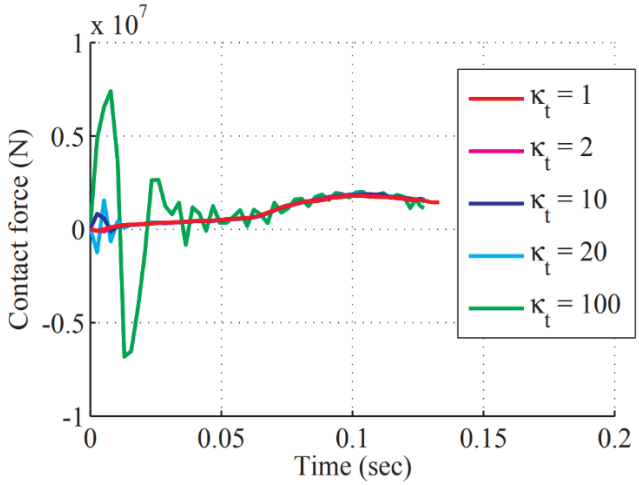

Figure 7. Abaqus results of contact forces as a parameter of time scaling factor: for higher scaling factor, it can be noticed that the kinetic energy dominates at the beginning but soon decays. Adopted from [23]

5. Results and Discussion

The coupled temperature-structure analyses were performed for the thermocline tanks of both Solar One Plant and the TEDS with the temperature boundary conditions discussed in Section 4. Investigations have been conducted on various model parameters used for the infinite rigidity and Drucker-Prager (DP) models. In this section, the simulation results of the thermal stresses and comparison with the experimental data obtained from Solar One thermocline tank are summarized. The insights into the effect of different modeling parameters for the infinite rigidity and DP models can be useful to support the insight into the experimental setup for TEDS TES facility and provide guidance for its later test plan.

5.1 Boundary conditions and model setup

To gain insights into the effect of mechanical boundary condition for thermal ratcheting analysis, the different boundary condition setup was tested to constrain the TES tank geometry. Mesh sensitivity study was also conducted to assure the convergence of the thermal stress simulation results while balancing the computational cost at the same time. What's more, the optimization of the time scaling factor was performed with the TES tank of Solar One plant using the Drucker-Prager (DP) model assumption.

5.1.1 Constraint (mechanical boundary condition)

During the structural/stress analysis, constraints define where and how the modeling geometry is fixed during the heating and/or cooling cycle. In Abaqus simulation, this type of constraints is specified as mechanical boundary conditions as initial setup before sequential coupled thermal-stress analysis steps in the model setup processes. To get a reasonable and realistic result for the stress analysis, the constraint setting must be considered and investigated carefully to represent the real-world scenarios as much as possible. However, this might not be straightforward given the complexity of the connection between the TES tank geometry and its fixture base. In this light, some possible constraints which could potentially represent the TES tank fixture should be investigated, and the resultant stresses need to be compared with the experimental data for validation.

In order to investigate how the different constraint settings will affect the thermal stress analysis, Solar One plant geometry (shown in Figure 2) is chosen, and two different constraints are applied at the bottom part of the tank for testing:

i. Bottom plate being fixed in all (x, y, and z) directions: this simulates the fixture for the bottom surface of the TES tank on the floor.

ii. Bottom plane being fixed with its normal displacement direction, while the center of the bottom plane got fixed in all directions: this is loose constrains compared to the first one, the bottom surface of the tank is placed on the floor so that it can only expand horizontally without constraining its circumference.

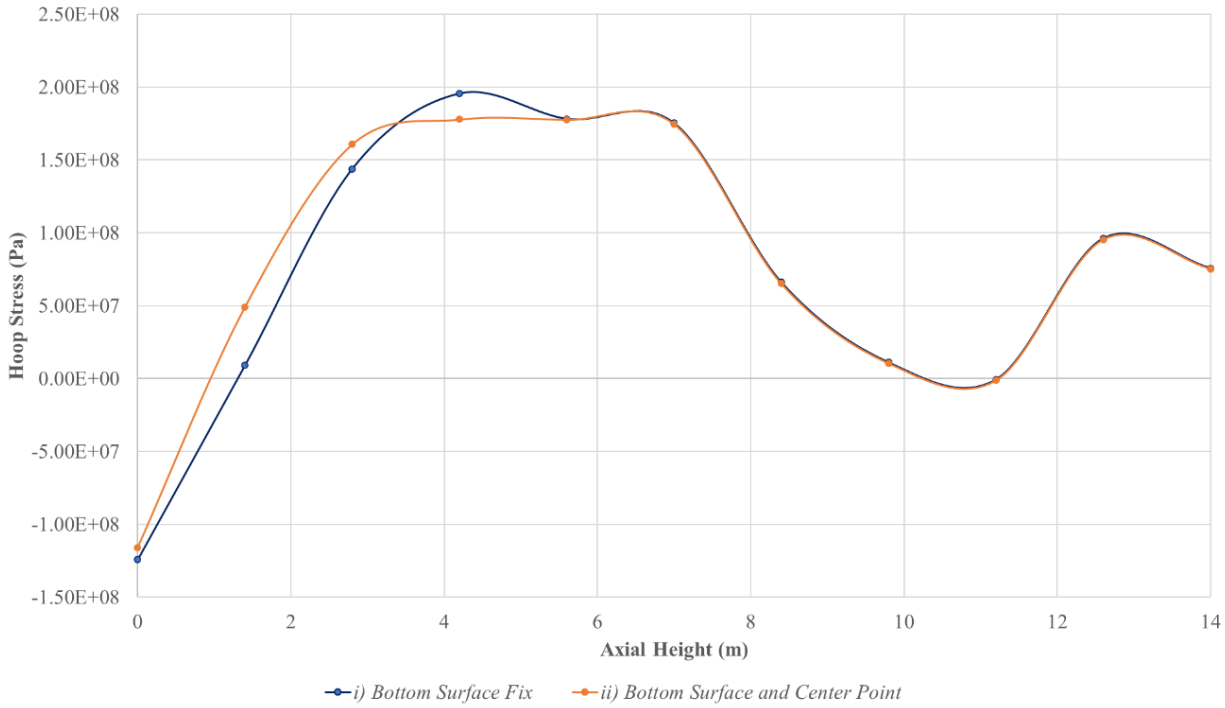

Figure 8. Simulated hoop stresses along the axial height of the Solar One tank with different constraints.

In Figure 8, the hoop stresses experienced on the outer surface of the Solar One TES tank are compared for the two constraining boundary conditions mentioned above. It can be noticed that the two different constraints applied to the bottom surface do not significantly affect the hoop stresses. Only some minor deviations are observed at the lower part of the tank, but the axial distribution of the hoop stresses is still dominated by the axial temperature boundary conditions applied during the heating and cooling period.

5.1.2 **Mesh independence study**

In order to balance the accuracy of the simulation results with the computational cost, mesh independence study was performed for the Solar One TES tank. Figure 9 shows the hoop stresses along the axial height of the TES tank evaluated with the infinite rigidity assumption using different mesh sizes.

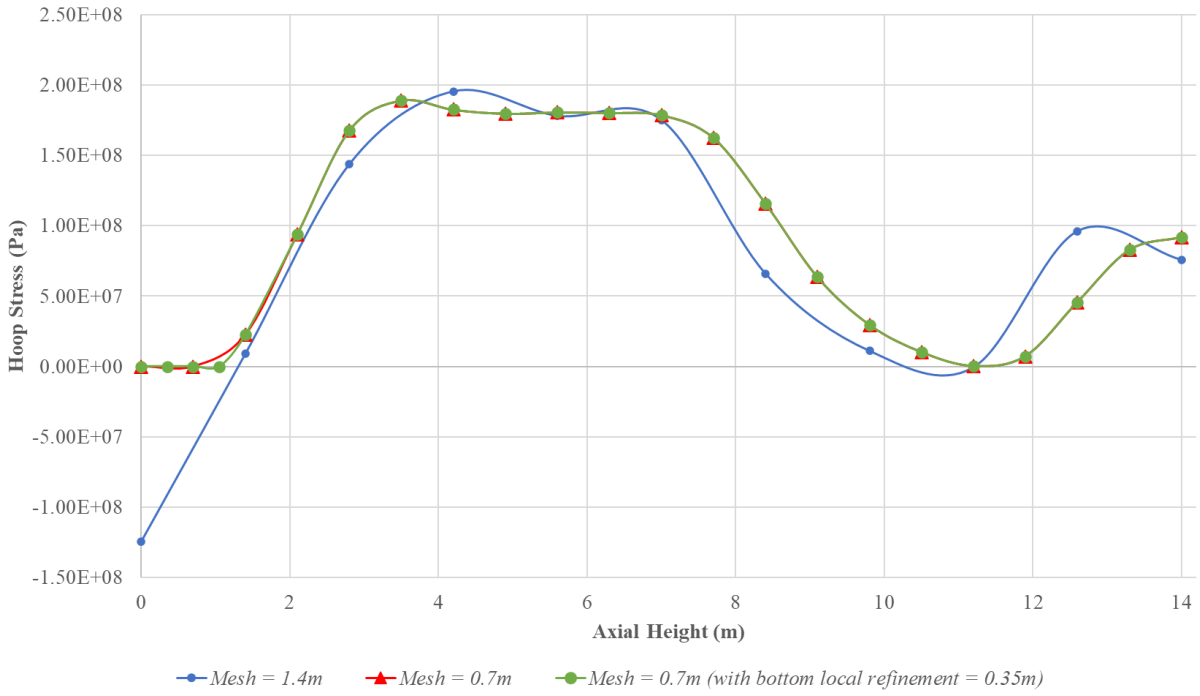

Figure 9. Simulated hoop stresses with different meshing setup.

All the simulation results shown in Figure 9 have a common maximum hoop stress value of around 180MPa. However, for the coarse mesh (mesh size=1.4m),the hoop stresses deviate substantially at the tank bottom from 0 to 1.4 m. This is because with the mesh base size of 1.4m, the bottom part of the tank from 0 to 1.4m, only has one mesh cell, therefore, the resulting hoop stress cannot be resolved properly at this region. When refining the mesh base size to 0.7m, the hoop stresses start to approach zero at the bottom part. The convergency can be noticed when refining the mesh base size to be 0.35m locally at the tank bottom region.

5.1.3 **Time scaling factor**

As mentioned in the previous section, Drucker-Prager (DP) model for the realistic simulation of the filler particle behavior requires the implementation of Abaqus/Explicit module. However, it is computationally expensive (for more than one-week physical time) to finish one 48-hour complete heating (24-hour) and cooling (24-hour) cycle with this approach. Therefore, the coupled temperature-structural analysis using DP model is performed by scaling the thermal loads and adjusting the thermal coefficient using Equation (1) and (2), to reduce the computational burden while maintaining the simulation repeatability and accuracy.

For the purpose of simplification and cost-efficiency, the TES tank for Solar One plant geometry is introduced with the DP modeling parameters discussed in Section 4.2.2. Three different time scaling factor κ = 100,000, 10,000 and 1,000 are used in the coupled temperature-structural analysis, and the resulting temperature and hoop stresses distributions are plotted in Figure 10 and Figure 11. It can be noticed that both temperature and hoop stress profiles along the TES tank axial height have quite similar magnitudes and distribution, only slight deviations can be observed for the stress profiles shown in Figure 11. However, according to the study shown in Figure 7 conducted by Hammelmüller and Zehetner [23], the results (shown in green curve) from choosing a relatively-large time scaling factor would have the

damping effect that requires a certain amount of iterations for the results to converge. Therefore, the time scaling factor κ = 10,000 is chosen to balance the accuracy and computational cost in this study, ensuring that the Abaqus simulation results will not be affected by the damping effect.

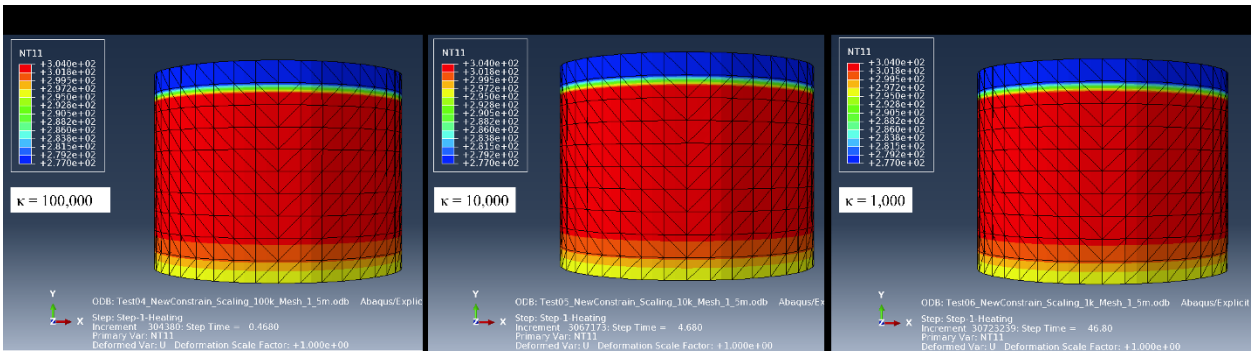

Figure 10. Simulated temperature distributions for Solar One TES tank with time scaling factor: (a) κ = 100,000, (b) κ = 10,000, and (c) κ = 1,000.

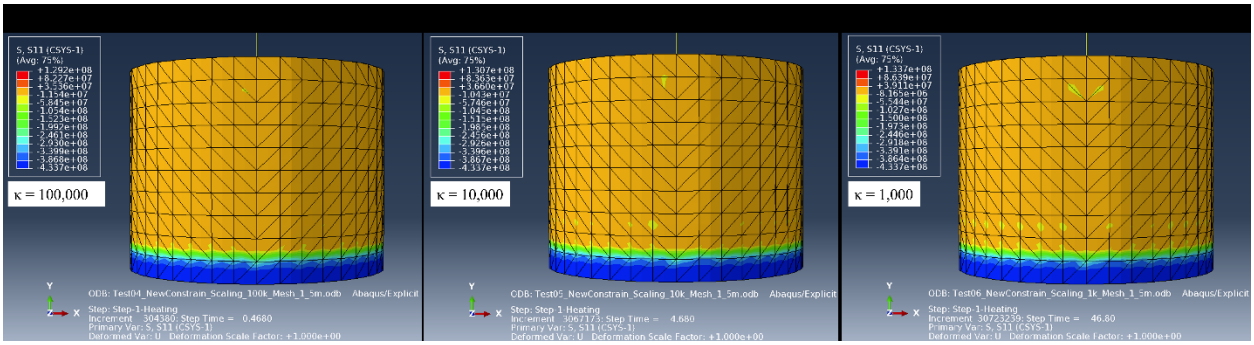

Figure 11. Simulated hoop stress distributions for Solar One TES tank with time scaling factor: (a) κ = 100,000, (b) κ = 10,000, and (c) κ = 1,000.

5.2 **Parametric investigations and validation**

According to the literature review, there is a clear knowledge gap for the thermomechanical analysis of packed-bed thermal energy storage tank, especially with respect to DP model. There are multiple parameters determining the tank and filler material properties that need to be investigated, and the parametric study of those modeling parameters will help understand their effects on thermal ratcheting process in the packed-bed TES tank. Given the temperature boundary conditions from the thermal analysis, we conducted the parametric study for the modeling parameters used in the stress models with the tank geometries of Solar One Plant as well as the TEDS facility. To outline the parametric study, Table 10 has summarized the parameters of interest for the current coupled temperature-structural analysis, including the tank material property, filler material properties, and the interaction parameters between the tank wall and the filler materials inside.

Table 10. Parametric study for Solar One plant and the TES tank of TEDS facility.

Case No.	Geometry		Model Setup		Tank Material Property		Tank-Filler Interaction		Filler Material Property			
	Solar One Plant	TEDS	Infinite Rigidity	DP Model	Thermal expansion coefficient		Wall-Filler friction coefficient		Internal angle of friction (deg)		Shear modulus (MPa)	
					1.3	1.48	0	0.5	34	60	25	75
1-1	✓		✓		✓		N/A		N/A		N/A	
1-2	✓			✓	✓			✓	✓		✓	
1-3	✓			✓	✓			✓	✓			✓
1-4	✓			✓		✓		✓	✓		✓	
1-5	✓			✓		✓		✓	✓			✓
1-6	✓			✓	✓			✓		✓	✓	
1-7	✓			✓	✓		✓			✓	✓	
1-8	✓			✓		✓		✓		✓	✓	
1-9	✓			✓		✓	✓			✓	✓	
2-1		✓	✓		✓		N/A		N/A		N/A	
2-2		✓	✓			✓	N/A		N/A		N/A	
2-3		✓		✓	✓			✓	✓			✓
2-4		✓		✓	✓			✓		✓		✓
2-5		✓		✓	✓		✓		✓			✓
2-6		✓		✓	✓		✓			✓		✓
2-7		✓		✓		✓		✓	✓			✓
2-8		✓		✓		✓		✓		✓		✓
2-9		✓		✓		✓	✓		✓			✓
2-10		✓		✓		✓	✓			✓		✓
2-11		✓		✓	✓		✓		✓		✓	
2-12		✓		✓		✓	✓		✓		✓	
2-13		✓		✓		✓		✓	✓		✓	

5.2.1 **Solar One Plant Analysis**

Using the Solar One TES tank geometry and the temperature profiles given by Flueckiger et al. [9] , Abaqus simulations were performed for the heating and cooling cycles with the infinite rigidity assumption as well as DP model. The model parameters of interest and the specific test cases for this study (case no. 1-x for Solar One) are summarized in Table 10. The simulation results are discussed as follows.

5.2.1.1 *Infinite rigidity assumption*

Figure 12 presents the hoop stress profile on the Solar One TES tank wall along the axial height, evaluated with the infinite rigidity assumption (Case no. 1-1). The simulated hoop stress distributions are then compared with the experimental data from Faas et al. [8] as well as the FEM analyses conducted by Flueckiger et al. [9] The simulation results show some differences at the bottom and top of the tank, The abaqus results predicts a slower increasing trend compared to the results presented in Fluckiger et al. Given the fact that the literature might use extremely high-resolved meshing scheme for both their coupled temperature-structural analysis, this deviation can potentially be caused by the numerical differences yielding from the different meshing setup.

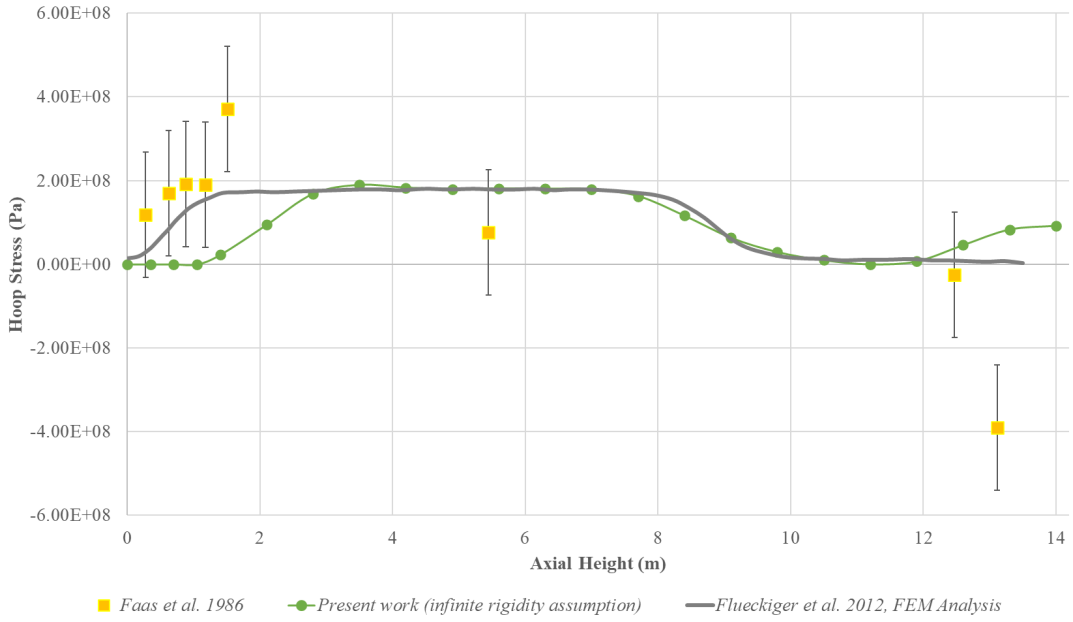

Figure 12. Simulated hoop stresses with the infinite rigidity assumption using Abaqus and compared with the experimental data from Faas et al. [8] as well as FEM simulation results from Flueckiger et al. [9]

In general, both the simulated hoop stresses show good agreements for the maximum magnitude of the hoop stresses. Except for two extreme datapoints measured by Faas et al. (which is located at about 1.5m and 13.11m in height), the Abaqus simulation shows reasonable agreements with the experimental data if considering the measurement uncertainties. In addition, given the fact there is noticeable discrepancy only at the bottom and top region of the tank shown in our present work, more investigations as future work should be performed for the possible differences in the constraint settings used to fix the tank bottom.

5.2.1.2 *DP model: Thermal expansion coefficient of tank material*

In Table 10, there are couple of comparison cases for different thermal expansion coefficient applied to the TES tank material for Solar one, such as Case no. 1-2 vs. 1-4, 1-3 vs. 1-5, 1-6 vs. 1-8 and 1-7 vs. 1-9. In this section, Case no. 1-2 vs. 1-4 is selected to discuss the effect of the tank wall thermal

expansion setting on thermal ratcheting (or hoop stress).

The simulated hoop stresses are plotted along the tank axial height for the two selected cases as shown in Figure 13. Using the Solar One TES tank geometry with DP modeling assumption, negligible differences can be noticed for the two thermal expansion coefficients. Table 11 shows the maximum magnitude of the axial hoop stresses at four azimuthal angles around the TES tank outer surface. Similar as the findings observed in Figure 13, the differences between these two cases are limited up to 1%. This indicates that the differences of the thermal expansion coefficient applied to the tank wall does not dominate the variation of the hoop stresses simulation with DP modeling.

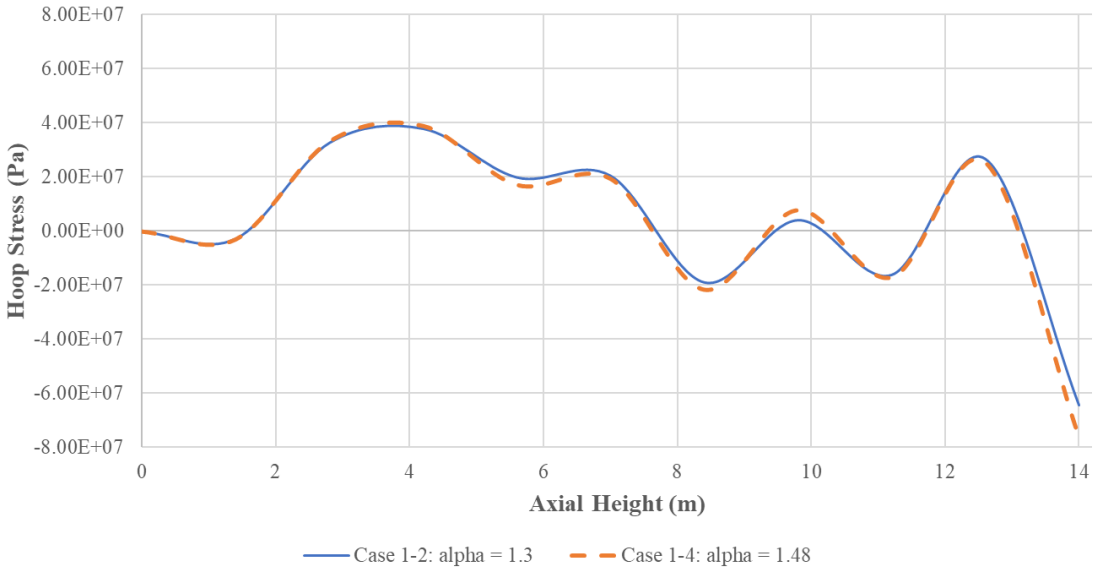

Figure 13. Simulated hoop stresses with different expansion coefficients in Case # 1-2 vs 1-4.

Table 11. The maximum hoop stresses along the tank height at various azimuthal angles around the tank outer surface for Case # 1-2 vs 1-4.

Case no.	Thermal expansion coefficient (m/m-K)	Max. Hoop Stresses (MPa) at Azimuthal Angle of			
		0°	90°	180°	270°
1-2	1.3e-05	37.17	42.56	34.72	38.84
1-4	1.48e-05	37.09	56.47	34.26	41.29

5.2.1.3 *DP model: Wall-Filler friction coefficient*

To evaluate the effect of wall-filler friction coefficient, two comparison cases are included in Table 10 for the Solar One TES tank, Case no. 1-6 vs. 1-7 and 1-8 vs. 1-9. In this section, Case no. 1-6 vs. 1-7 is selected to investigate the effect of the wall-tank interaction setting on thermal ratchetting.

During the discharging (or cooling) cycle, a larger value of the wall-filler friction coefficient should lead to the resistance of filler rearrangements, therefore, inducing higher hoop stress values. The

comparison with different friction coefficients plotted in Figure 14 has indicated that the Abaqus DP modeling predicts reasonable results. Agreeing with the research work conducted by Cho et al. [24], the maximum hoop stresses shown in Table 12 at different azimuthal angles are about 20% lower with a lower wall-filler friction coefficient. What's more, it can be noticed that the simulated hoop stress values, summarized in Table 12, are significantly lower than the carbon steel's yield strength limit (which is 414 MPa [9]), confirming the structural integrity during its normal operation.

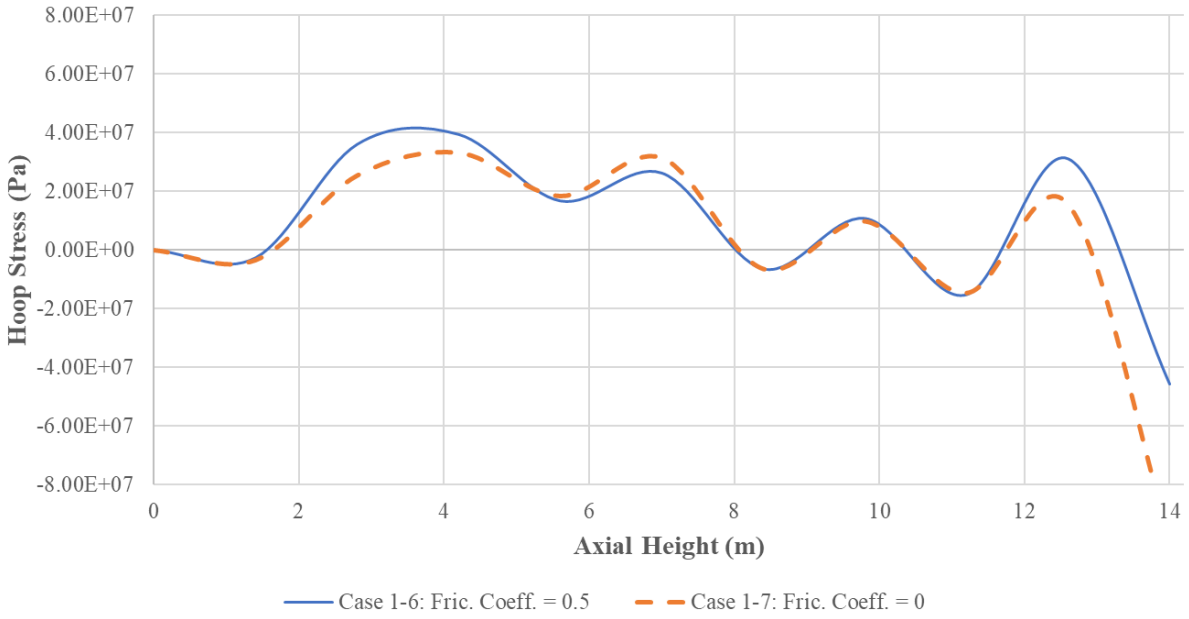

Figure 14. Simulated hoop stresses with different wall-filler friction coefficients in Case # 1-6 vs 1-7.

Table 12. The maximum hoop stresses along the tank height at various azimuthal angles around the tank outer surface for Case # 1-6 vs 1-7.

Case no.	Wall-Filler Friction Coefficient	Max. Hoop Stresses (MPa) at Azimuthal Angle of			
		0°	90°	180°	270°
1-6	0.5	41.16	45.50	37.95	41.53
1-7	0	38.95	36.67	31.06	33.65

5.2.1.4 *DP model: Internal angle of friction for filler material*

The comparison between Case no. 1-4 and 1-8 shown in Table 10 is aimed to investigate the effect of internal friction angle of the filler material for the Solar One TES tank when using the DP model.

As pointed out in the research performed by Cho et al. [24], the filler behavior depends on the initial packing states. It indicates that a higher friction angle could yield higher or lower hoop stress value highly depending on the filler materials' initial arrangement. If the filler beds are initially packed flat in the tank, there will be more filler beds to slide down and fill the gap during the charging process when increasing

the friction angle. Then, this will result in a larger hoop stress on the tank wall during the following discharge cycle.

The Abaqus simulation results shown in Figure 15 and Table 13 reproduce this physics properly, resulting in greater hoop stress values from a larger angle of friction. This indicated that the filler materials were indeed packed evenly at the very beginning of the model setup with the larger value of internal friction angle.

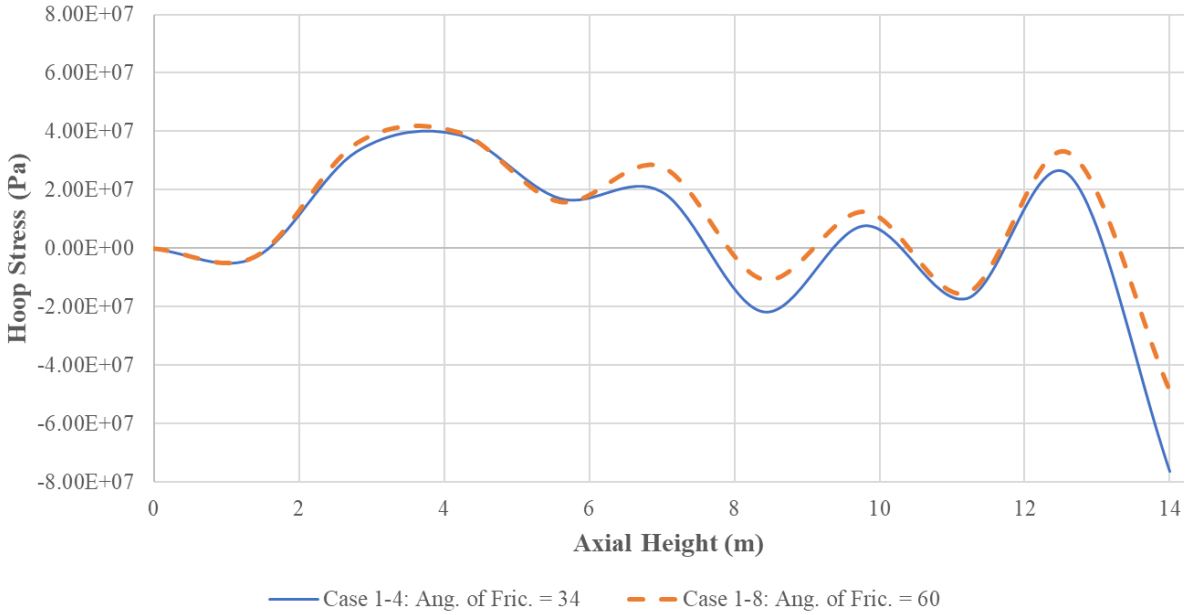

Figure 15. Simulated hoop stresses with different internal angle of friction of filler material in Case # 1-4 vs 1-8.

Table 13. The maximum hoop stresses along the tank height at various azimuthal angles around the tank outer surface for Case # 1-4 vs 1-8.

Case no.	Internal Angle of Friction	Max. Hoop Stresses (MPa) at Azimuthal Angle of			
		0°	90°	180°	270°
1-4	34°	37.09	56.47	34.25	41.29
1-8	60°	41.71	65.41	37.87	43.35

5.2.1.5 *DP model: Shear modulus of filler material*

Shear modulus should be specified in the DP model to represent the filler bed motion inside the TES tank during the charge and discharge cycles. Defined as the ratio of shear stress to shear strain, a smaller shear modulus value indicates a solid is softer or more flexible. The comparison case between Case # 1-2 and 1-3 shown in Table 10 is to investigate the effect of shear modulus on thermal ratcheting process when using DP model (Case # 1-4 vs 1-5 can be another case to investigate if interested).

Filler bed inside the TES tank will experience two steps involving shear mechanism during the whole process: the first one is the re-distribution step axially due to gravity during the charge cycle, and the other is the contraction step during the discharge cycle. The resultant hoop stress profile at the end of the discharge cycle is a combined reflection from the two above steps. As shown in both Figure 16 and Table 14, the case with a lower shear modulus value results in a higher hoop stress at the end of the discharge cycle. This indicates that, with a smaller shear modulus, the filler bed fills the gap during the charging process and then reacts better against the centripetal contraction process during the discharge cycle. Due to the limited literature database available for the shear modulus of the materials used for TES filler beds, this could be a great research topic to investigate and refine the DP modeling as future work.

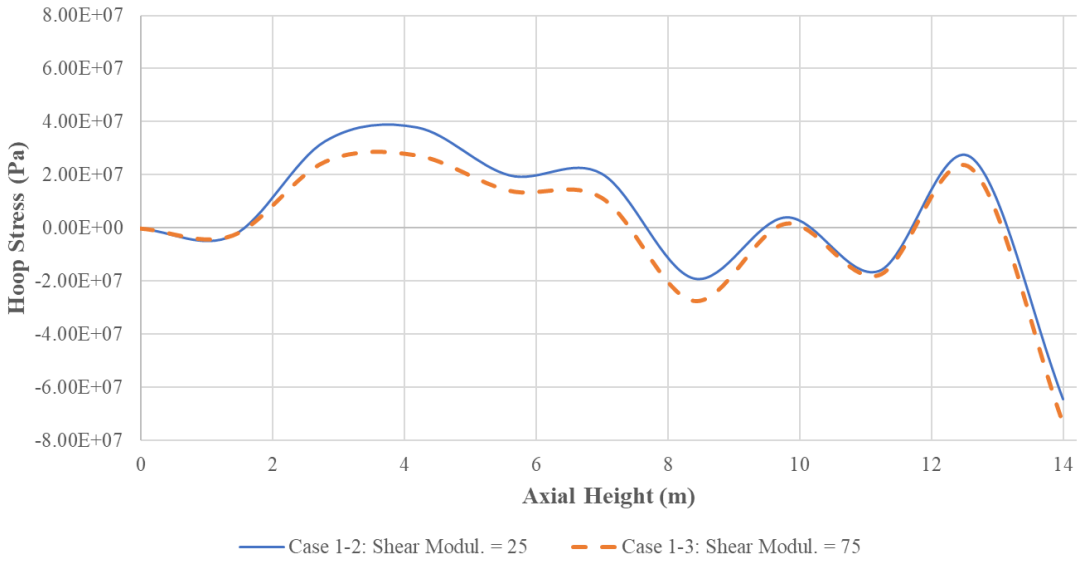

Figure 16. Simulated hoop stresses with different shear modulus of filler material in Case # 1-2 vs 1-3.

Table 14. The maximum hoop stresses along the tank height at various azimuthal angles around the tank outer surface for Case # 1-2 vs 1-3.

Case no.	Shear Modulus (MPa)	Max. Hoop Stresses (MPa) at Azimuthal Angle of			
		0°	90°	180°	270°
1-2	25	37.17	42.56	34.72	38.84
1-3	75	29.65	38.05	27.59	29.53

5.2.2 **TEDS TES Tank Analysis**

Based on the TEDS TES tank geometry and the associated thermal analysis described in Section 4.1, thermal ratcheting analysis was performed during the charge and discharge cycles of the thermocline tank for TEDS. Case no. 2-1 to 2-13 in Table 10 summarized the specific simulation cases performed in this study. The model parametric study results were discussed in the following subsections.

5.2.2.1 *Infinite rigidity: Thermal expansion coefficient of tank material*

Similar to the study with Solar One TES tank (section 5.2.1.1), the infinite rigidity assumption is applied to the TEDS TES tank geometry for the Case # 2-1 vs 2-2 shown in Table 10. Same as the infinite rigidity model applied to Solar One TES tank, the mesh nodes at the inner side of the TEDS TES tank are set to expand freely with all the other nodes during the charge cycle but are fixed during the discharge cycle.

The axial hoop stress profiles at the outer surface of the TEDS tank are plotted in Figure 17 with two thermal expansion coefficient settings for the tank wall material. With the infinite rigidity model assumption, the hoop stress at the end of the discharge cycle can be expressed as , where is the thermal expansion coefficient of tank material, the tank material's Young's modulus, and operating temperature differential along the points of interest in the system. Therefore, a larger thermal expansion coefficient results in higher hoop stress profile along the tank axial height.

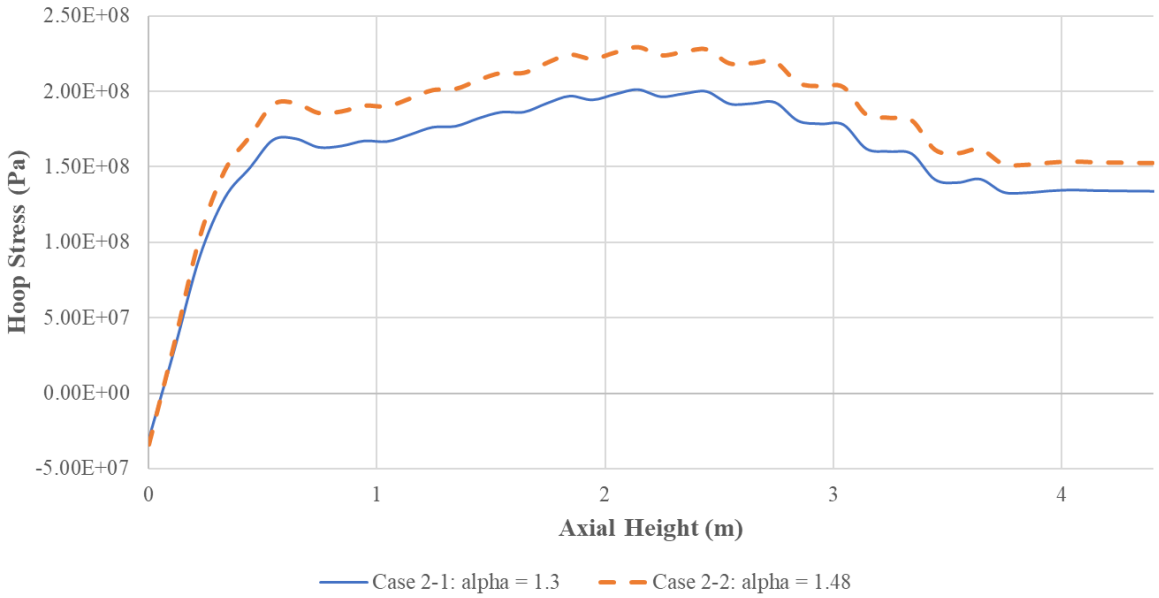

Figure 17. Simulated hoop stresses with different thermal expansion coefficient in TEDS Case # 2-1 vs 2-2 (infinite rigidity assumption).

The maximum hoop stresses along the tank axial height are summarized in Table 15 for both cases using different thermal expansion coefficient. Since the infinite rigidity assumption is a strict constrain scenario, The maximum hoop stresses are expected to be higher than the results from DP modeling. Table 15 shows that the maximum hoop stresses evaluated at different azimuthal angles of the tank outer surface are linearly proportional (~13.85% increment) to the thermal expansion settings. The maximum hoop stress shown in Table 15, 231.07 MPa, is about 200 MPa lower than the carbon steel's yield strength limit (414 MPa). This indicates that with those thermal expansion properties the TEDS TES tank should operate safely and will not experience any risk of plastic deformation during the normal charging and discharging processes.

Table 15. The maximum hoop stresses along the tank height at various azimuthal angles around the tank outer surface for TEDS Case # 2-1 vs 2-2.

Case no.	Thermal expansion coefficient (m/m-K)	Max. Hoop Stresses (MPa) at Azimuthal Angle of			
		0°	90°	180°	270°
2-1	1.3e-05	202.12	202.96	201.66	200.35
2-2	1.48e-05	230.11	231.07	229.58	228.09

5.2.2.2 *DP model: Thermal expansion coefficient of tank material*

Table 10 includes a couple of comparison cases using DP model with different thermal expansion coefficients of TES tank wall material, such as Case no. 2-3 vs 2-7, 2-4 vs 2-8, 2-5 vs 2-9 and 2-6 vs 2-10. In this section, the study between Case # 2-3 vs 2-7 is selected to discuss the effect of the thermal expansion setting on thermal ratcheting of the TEDS TES tank.

Due to the implementation of DP modeling scheme with looser constraints on the tank wall nodes during the discharge period, the hoop stress profiles presented in Figure 18 show a significantly lower magnitude compared to the stresses evaluated with infinite rigidity assumption. But, still as expected, Case # 2-7 with a higher thermal expansion coefficient for the tank material still results in higher stress values than the results of Case # 2-3. Besides the high stresses at the tank bottom and top (because these locations endure the largest temperature changes for thermal analysis results shown in Figure 6 during the heating and then cooling cycle), we can also notice that the region of a high hoop stress is observed at tank heights between 0.67 and 1.34m. This corresponds to the bottom flow distributor location shown in Figure 2 where the filler materials are expected to re-distribute due to gravity effect by the end of the charge cycle, therefore, the hoop stresses are induced by the resisting force from the filler beds to the tank wall. Since the case comparison will not be only dominated by the thermal expansion coefficient of the tank but it is now a combined effect with the filler bed interactions as well, the maximum hoop stresses tabulated in Table 16 increase about 30%, which is larger than the 13.85% increment of the thermal expansion coefficient.

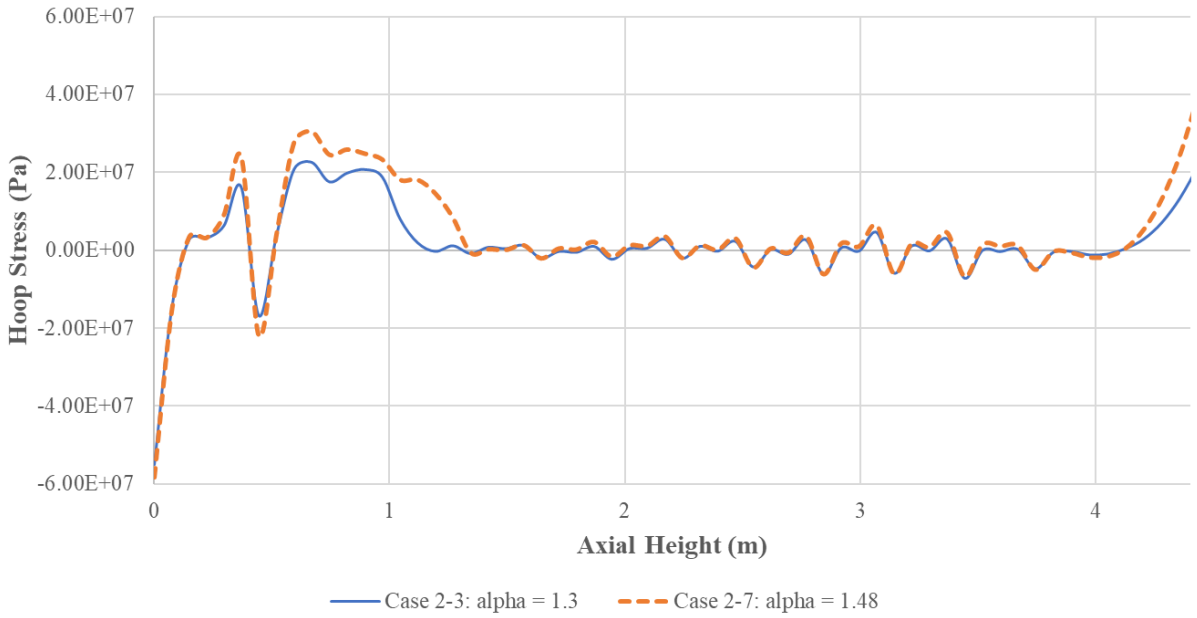

Figure 18. Simulated hoop stresses with different thermal expansion coefficient (DP modeling assumption) in TEDS Case # 2-3 vs 2-7.

Table 16. The maximum hoop stresses along the tank height at various azimuthal angles around the tank outer surface for TEDS Case # 2-3 vs 2-7.

Case no.	Thermal expansion coefficient (m/m-K)	Max. Hoop Stresses (MPa) at Azimuthal Angle of			
		0°	90°	180°	270°
2-3	1.3e-05	23.04	24.00	23.22	20.28
2-7	1.48e-05	31.20	29.42	31.11	30.32

5.2.2.3 *DP model: Wall-Filler friction coefficient*

To evaluate the effect of friction between tank wall and porous bed in the TEDS TES tank, simulations were performed with several different values of wall-filler friction coefficients. The specific test cases are given in Table 10: Case no. 2-3 vs 2-5, 2-4 vs 2-6, 2-7 vs 2-9 and 2-8 vs 2-10. In this section, Case no. 2-7 vs. 2-9 is selected to discuss the effect of the wall-tank interaction setting on thermal ratcheting.

As shown in Figure 19, the case with a larger wall-filler friction coefficient results in a larger peak magnitude at the bottom flow distribution region, but the hoop stress decades quicker. Similar with the analysis for Solar One DP modeling shown in Figure 14, a larger value of the wall-filler friction coefficient is expected to lead to the resistance of filler rearrangements during the discharge cycle, therefore, inducing higher hoop stress values. However, the filler beds which re-distribute due to gravity during the heating process will tend to remain staying there with the setting of a larger friction coefficient and exert forces to the tank wall during the discharge period. Table 17 presents the maximum hoop stresses evaluated along the tank wall for both cases. The maximum stresses at different azimuthal angles

are observed to all stay within the carbon steel's yield strength limit (414 MPa).

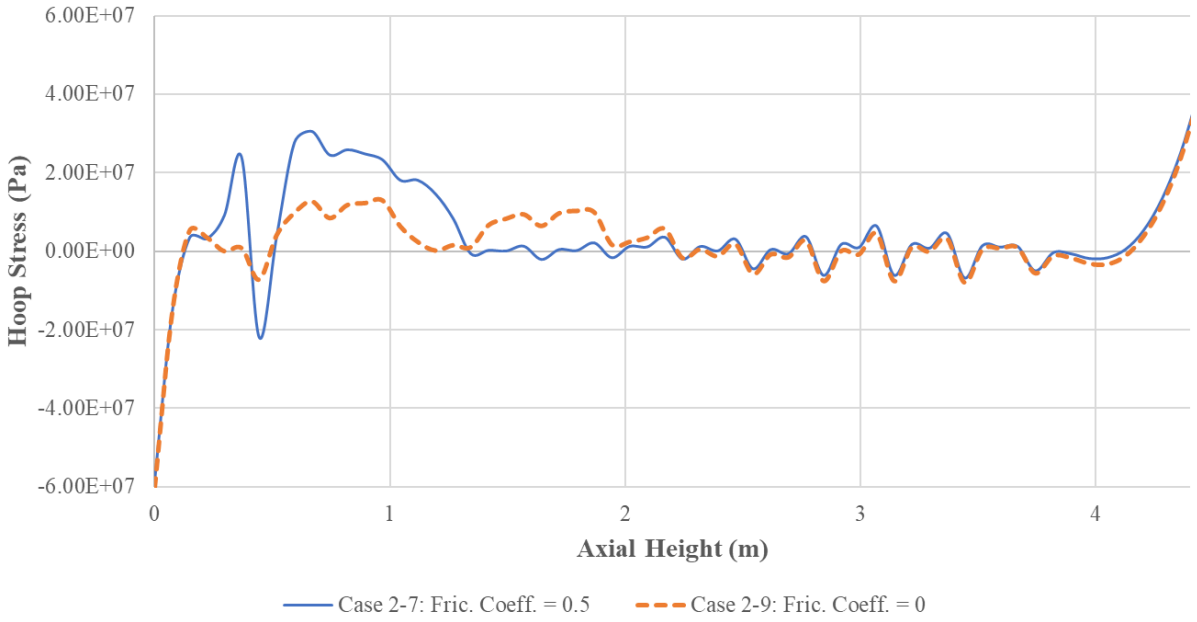

Figure 19. Simulated hoop stresses with different wall-filler friction coefficients in TEDS Case # 2-7 vs 2-9.

Table 17. The maximum hoop stresses along the tank height at various azimuthal angles around the tank outer surface for TEDS Case # 2-7 vs 2-9.

Case no.	Wall-Filler Friction Coefficient	Max. Hoop Stresses (MPa) at Azimuthal Angle of			
		0°	90°	180°	270°
2-7	0.5	31.20	29.42	31.11	30.32
2-9	0	17.96	23.95	26.33	24.22

5.2.2.4 *DP model: Internal angle of friction for filler material*

There are several case comparisons shown in Table 10 to investigate the effect of different internal angle of friction for filler material with the DP modeling assumption, including Case no. 2-3 vs 2-4, 2-5 vs 2-6, 2-7 vs 2-8 and 2-9 vs 2-10. In this section, the comparison between Case # 2-9 and 2-10 is discussed.

As mentioned previously, a higher friction angle could yield either higher or lower hoop stresses at the end, but this process is highly dependent on the filler materials' initial arrangement. If the filler bed is initially packed flat in the tank, there will be more filler materials to slide downward due to gravity effect and fill the gap during the charging process, therefore, resulting in a larger hoop stress on the tank wall during the following discharge cycle, vice versa. The hoop stresses presented in Figure 20 and Table 18 show greater hoop stress values for the case with a larger angle of friction. Similar to the discussion for

the Solar One TES tank analysis in Section 5.2.1.4, this implied that the filler materials were indeed packed evenly at the very beginning of the model setup.

However, given the slight differences of the maximum hoop stresses for both Solar One Plant and TEDS results shown in Table 13 and Table 18 , as well as its nature of uncertainty with the filler bed initial packing status, the internal angle of friction is not considered a dominating parameter that affects the hoop stress in the DP model and unlikely to be controlled during the actual experimental study.

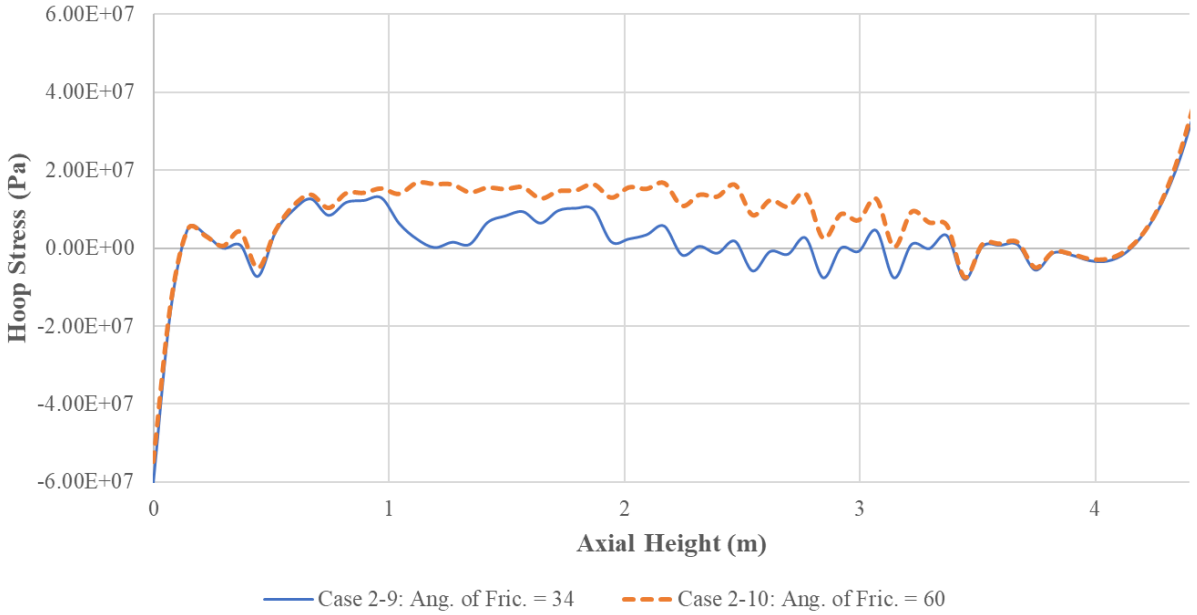

Figure 20. Simulated hoop stresses with different internal angle of friction of filler material in TEDS Case # 2-9 vs 2-10.

Table 18. The maximum hoop stresses along the tank height at various azimuthal angles around the tank outer surface for TEDS Case # 2-9 vs 2-10.

Case no.	Internal Angle of Friction	Max. Hoop Stresses (MPa) at Azimuthal Angle of			
		0°	90°	180°	270°
2-9	34°	17.96	23.95	26.33	24.22
2-10	60°	25.54	23.09	25.91	23.99

5.2.2.5 *DP model: Shear modulus of filler material*

To represent the filler beds motions inside the tank during the charge and discharge cycles, shear modulus, defined as the ratio of shear stress to shear strain, is incorporated in the DP modeling setup for TEDS TES tank as well. The investigation for the shear modulus involves Case no. 2-5 vs 2-11, 2-9 vs 2-12 and 2-7 vs 2-13 in Table 10, and the comparison for Case # 2-5 vs 2-11 is selected for discussion in this section.

According to its definition, a smaller shear modulus value indicates a solid is softer or more flexible. As discussed in the previous study with Solar One plant, the hoop stress profile in the end of the discharge cycle is a combined reflection from the two steps: the re-distribution step due to gravity during the charge cycle, and the contraction step during the discharge cycle. The selected cases with two different shear moduli have a quite similar trend and magnitude of the hoop stresses as shown in Figure 21, except for the region (from 0.67 to 1.34m in the tank axial direction) near the bottom flow distributor of the TEDS TES tank. Unlike the finding with the Solar One plant, the TEDS case with a lower shear modulus setting of 25MPa shows lower maximum hoop stresses, and this can be also confirmed with the comparison shown in Table 19. This difference may be due to the differences in tank geometry and shape between TEDS and Solar One TES tanks (e.g., tank height-to-diameter ratio), affecting the re-distribution of filler materials and the contraction rate. Given the fact that there are still clear knowledge gaps for the TES filler media properties, this could be an interesting topic to refine the thermal stress analysis with DP modeling as a future work plan.

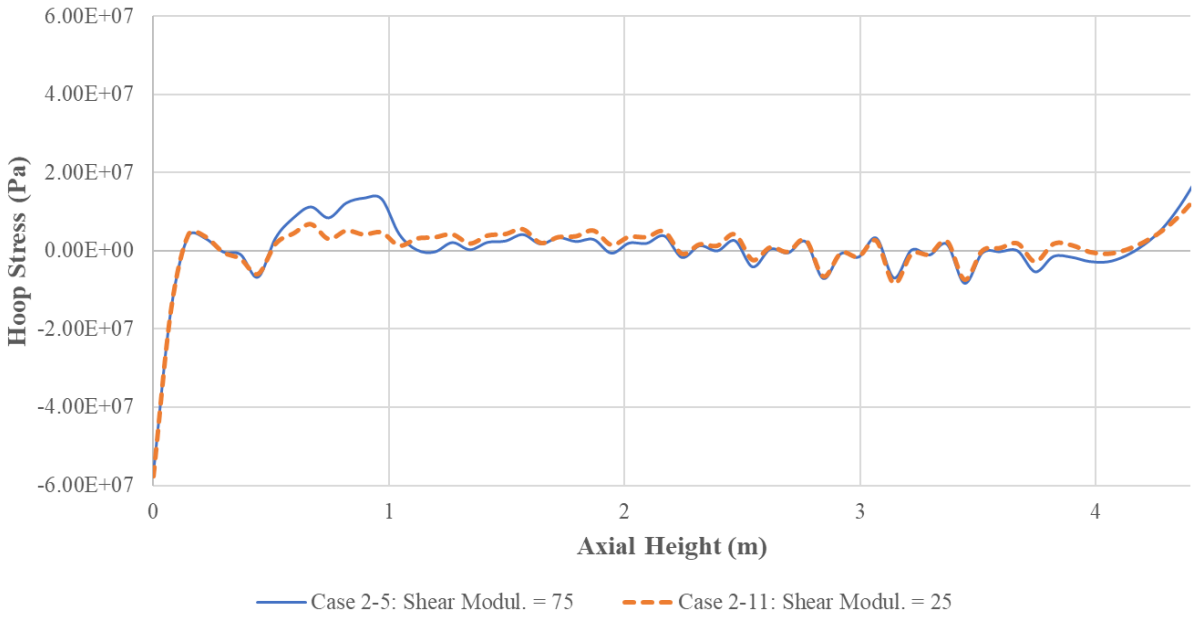

Figure 21. Simulated hoop stresses with different shear modulus of filler material in TEDS Case # 2-5 vs 2-11.

Table 19. The maximum hoop stresses along the tank height at various azimuthal angles around the tank outer surface for TEDS Case # 2-5 vs 2-11.

Case no.	Shear Modulus (MPa)	Max. Hoop Stresses (MPa) at Azimuthal Angle of			
		0°	90°	180°	270°
2-5	75	14.11	14.16	14.58	11.94
2-11	25	8.87	8.36	10.19	9.59

6. Conclusions

This report discussed the numerical modeling methods for thermal ratcheting analysis of packed-bed thermocline tank, involving both thermal and structural modeling and simulation. The experimental data obtained from various design characteristics of packed-bed thermocline tanks, including TEDS TES tank, were used to validate thermal and mechanical models developed in this study.

In the validation study of the thermal model, the transient thermal propagation through the packed-bed thermocline tanks was predicted well during the charge and discharge cycles of the thermocline tanks, but a larger discrepancy was observed between the thermal model predictions and the TEDS experimental data. This discrepancy appears to be mainly due to the uncertainty of boundary conditions given from the experiment. Therefore, based on the comparative study between the thermal model predictions and experimental data, potential improvements were suggested for the TEDS future experiment for more precise validation study.

For the structural (or stress) analysis, the temperature profiles obtained from thermal analysis or experimental data were employed as the boundary conditions, and Abaqus was utilized to perform the coupled temperature-structural analysis for the TES tanks of Solar One Plant and INL TEDS facility. Both tank geometries were implemented in Abaqus with two different modeling schemes: infinite rigidity model which strictly fixed the tank inner side during the discharge cycle; and DP model that simulated a more realistic filler bed behavior as a continuum and its interaction with the tank wall. To investigate the effect of various modeling parameters on thermal ratcheting analysis, a comprehensive model parametric study was performed with both modeling approaches for both Solar One and TEDS thermocline tanks. The model parameters discussed include the tank material properties, filler material properties, and the interaction parameters between the tank wall and the filler material.

Infinite rigidity assumption was firstly applied to Solar One plant, and the results showed a good match for the maximum hoop stress magnitude compared with and the experimental database from Faas et al [8] and the simulation performed by Flueckiger et al. [9]. However, large discrepancies for the stress increasing slope were observed locally at the bottom of the tank, primarily due to the uncertainty of the TES tank constraint settings given from the experiment. It was also noticed that the maximum hoop stresses were evaluated as linearly proportional to the thermal expansion coefficients under the infinite rigidity modeling scheme.

For DP model with a more complicated scenario for filler-tank interactions, it was observed that the maximum hoop stresses had a larger increasing rate than the thermal expansion coefficients of the tank material. Secondly, a larger wall-filler friction coefficient always resulted in a larger peak of hoop stresses at the bottom flow distribution region, but the stresses decayed more quickly. This is primarily caused by the effect of filler re-distribution during the charging period. What's more, the internal angle of friction for the filler material was found not to be a dominant parameter in the DP modeling. Finally, the effect from the shear modulus of the filler material properties will need more investigation given the fact that limited database could be found in the existing literature. The geometry effect of the TES tank, e.g., tank height-to-diameter ratio (H/D) should be also investigated in the future work.

Regarding the thermal ratcheting potential of the TEDS thermocline tank, both modeling methods predicted the hoop stress values that were significantly lower than the yield strength of the carbon steel used for TEDS thermocline tank wall. This indicates that the TEDS TES tank will hold its structural integrity during the normal operating cycles. It is noted, however, there are knowledge gaps for the modeling parameters used for the filler material properties with DP model and the constraint settings for the TES tank. These are the potential future work needed to improve the model prediction accuracy for the advanced thermal ratcheting analysis and better support the TES design and experimental work. All the simulation files have been documented on INL HPC cluster, and those can be used for future analysis research to improve the thermal ratcheting model accuracy and provide guidance to design the

experimental test matrix for TEDS.

7. Acknowledgement

The authors would like to acknowledge the financial support by INL's Integrated Energy Systems (IES) Program under U.S. Department of Energy Office of Nuclear Energy. This research also made use of the resources of the High Performance Computing (HPC) Center at INL, which is supported by the Office of Nuclear Energy of the U.S. Department of Energy and the Nuclear Science User Facilities under Contract No. DE-AC07-05ID14517.

Reference

[1] S. M. Bragg-Sitton *et al.*, "Integrated energy systems: 2020 roadmap," Idaho National Lab.(INL), Idaho Falls, ID (United States); Oak Ridge …, 2020.

[2] M. D. A. Co. and C. U. Huntington Beach, "10 MWe Solar Thermal Central Receiver Pilot Plant Mode 5 Charging Only Acceptance Test Procedure 1150," SAND84-8183, 1984.

[3] C. M. Stoots, A. Duenas, P. Sabharwall, J. E. O'Brien, J. S. Yoo, and S. M. Bragg-Sitton, "Thermal Energy Delivery System Design Basis Report," Idaho National Lab.(INL), Idaho Falls, ID (United States); Oregon State Univ …, 2018.

[4] T. Esence, A. Bruch, J.-F. Fourmigué, and B. Stutz, "A versatile one-dimensional numerical model for packed-bed heat storage systems," *Renewable Energy,* vol. 133, pp. 190-204, 2019.

[5] J. E. Pacheco, S. K. Showalter, and W. J. Kolb, "Development of a molten-salt thermocline thermal storage system for parabolic trough plants," (in English), *J Sol Energ-T Asme,* vol. 124, no. 2, pp. 153-159, May 2002, doi: 10.1115/1.1464123.

[6] T. J. Morton, "Thermal Energy Distribution System (TEDS) Startup and Commissioning," Idaho National Lab.(INL), Idaho Falls, ID (United States), 2021.

[7] L. Radosevich, "Final report on the power production phase of the 10MWe solar central receiver pilot plant," *SAND87-8022. Sandia National Laboratories,* 1988.

[8] S. E. Faas, L. R. Thorne, E. A. Fuchs, and N. D. Gilbertsen, "10 MWe Solar Thermal Central Receiver Pilot Plant: thermal storage subsystem evaluation - Final report," SAND86-8212, 1986.

[9] S. M. Flueckiger, Z. Yang, and S. V. Garimella, "Thermomechanical simulation of the solar one thermocline storage tank," *Journal of solar energy engineering,* vol. 134, no. 4, 2012.

[10] S. Novascone, B. Spencer, J. Hales, and R. Williamson, "Evaluation of coupling approaches for thermomechanical simulations," *Nuclear Engineering and Design,* vol. 295, pp. 910-921, 2015.

[11] J. T. Van Lew, P. Li, C. L. Chan, W. Karaki, and J. Stephens, "Analysis of heat storage and delivery of a thermocline tank having solid filler material," *Journal of solar energy engineering,* vol. 133, no. 2, p. 021003, 2011.

[12] G. Nellis and S. Klein, *Heat transfer*. Cambridge university press, 2008.

[13] H. E. R. Center, "Solar Pilot Plant, Phase I. Preliminary design report. Volume I. Executive overview (approved). CDRL item 2. [10 MW; Barstow, California].", SAN1109-8/1, 1977.

[14] I. González, C. D. Pérez-Segarra, O. Lehmkuhl, S. Torras, and A. Oliva, "Thermo-mechanical parametric analysis of packed-bed thermocline energy storage tanks," *Applied energy,* vol. 179, pp. 1106-1122, 2016.

[15] A. Petruzzi, F. D'Auria, A. D. Crecy, P. Bazin, and S. B. e. al., "BEMUSE Programme. Phase 2 report (re-analysis of the ISP-13 exercise, post test analysis of the LOFT L2-5 experiment)," 2006, vol. NEA/CSNI/R(2006)2.

[16] R. G. Munro, "Evaluated material properties for a sintered alpha-alumina," (in English), *J Am Ceram Soc,* vol. 80, no. 8, pp. 1919-1928, Aug 1997. [Online]. Available: <Go to ISI>://WOS:A1997XQ33100001.

[17] "Abaqus FEA, SIMULIA website. https://www.3ds.com/products-services/simulia/products/abaqus/." (accessed April, 2022).

[18] D. C. Drucker and W. Prager, "Soil mechanics and plastic analysis or limit design," *Quarterly of applied mathematics,* vol. 10, no. 2, pp. 157-165, 1952.

[19] I. González, O. Lehmkuhl, C. Pérez-Segarra, and A. Oliva, "Dynamic thermoelastic analysis of thermocline-like storage tanks," *Energy Procedia,* vol. 69, pp. 850-859, 2015.

[20] B. D. Iverson, S. J. Bauer, and S. M. Flueckiger, "Thermocline Bed Properties for Deformation Analysis," *Journal of Solar Energy Engineering,* vol. 136, no. 4, 2014.

[21] Altair, "Altair Engineering RADIOSS Theory Manual, 14.0 Version, Large Displacement Finite Element Analysis," ed: Altair Engineering, Inc. Troy, MI, USA, 2015.

[22] "Abaqus/Explicit, SIMULIA website. https://www.3ds.com/products-services/simulia/products/abaqus/abaqusexplicit/." (accessed April, 2022).
[23] F. Hammelmüller and C. Zehetner, "Increasing numerical efficiency in coupled Eulerian-Lagrangian metal forming simulations," in *COMPLAS XIII: proceedings of the XIII International Conference on Computational Plasticity: fundamentals and applications*, 2015: CIMNE, pp. 727-733.
[24] S.-B. Cho, J. S. Yoo, K. L. Frick, and S. M. Bragg-Sitton, "Thermomechanical Analysis of Packed-Bed Thermal-Energy Storage Tanks: A Study of Design Parameters Affecting Thermal Ratcheting under Thermal Cycling Conditions " presented at the 19th International Topical Meeting on Nuclear Reactor Thermal Hydraulics (NURETH-19), Brussels, Belgium, 2022.